Geophys. J. Int. (1995) **122,** 899–924

Deep structure of the northern Kerguelen Plateau and hotspot-related activity

Philippe Charvis,[1] Maurice Recq,[2] Stéphane Operto[3] and Daniel Brefort[4]

[1]*ORSTOM (UR 14), Observatoire Océanologique de Villefranche-sur-mer, BP 48, 06230 Villefranche-sur-mer, France*

[2]*Domaines océaniques (URA 1278 du CNRS & GDR 'GEDO'), UFR des Sciences et Techniques, Université de Bretagne Occidentale, BP 809, 6 Avenue Le Gorgeu, 29285 Brest Cedex, France*

[3]*Laboratoire de Géodynamique sous-marine, GEMCO, (URA 718 du CNRS), Observatoire Océanologique de Villefranche-sur-mer, BP 48, 062320 Villefranche-sur-mer, France*

[4]*Institut de Physique du Globe de Paris, Laboratoire de Sismologie (LA 195 du CNRS), Boîte 89, 4 place Jussieu, 75252 Paris Cedex 05, France*

Accepted 1995 March 10. Received 1995 March 10; in original form 1993 June 16

SUMMARY

Seismic refraction profiles were carried out in 1983 and 1987 throughout the Kerguelen Isles (southern Indian Ocean, Terres Australes & Antarctiques Françaises, TAAF) and thereafter at sea on the Kerguelen–Heard Plateau during the MD66/KeOBS cruise in 1991. These profiles substantiate the existence of oceanic-type crust beneath the Kerguelen–Heard Plateau stretching from 46°S to 55°S, including the archipelago. Seismic velocities within both structures are in the range of those encountered in 'standard' oceanic crust. However, the Kerguelen Isles and the Kerguelen–Heard Plateau differ strikingly in their velocity–depth structure. Unlike the Kerguelen Isles, the thickening of the crust below the Kerguelen–Heard Plateau is caused by a 17 km thick layer 3. Velocities of 7.4 km s^{-1} or so within the transition to mantle zone below the Kerguelen Isles are ascribed to the lower crust intruded and/or underplated by upper mantle material. The crust–mantle boundary below the Kerguelen–Heard Plateau is abrupt and devoid of any underplated material. The difference in structure between the northern edge of the Kerguelen Plateau (including the archipelago) and the Kerguelen–Heard Plateau may be related to variability of the time-dependent hotspot activity. The Kerguelen–Heard Plateau was emplaced during the Cretaceous time (110 Ma) when the volcanic output rate of the Kerguelen Plateau and the Ninetyeast Ridge was high (as well as high potential temperature). The northernmost Kerguelen Plateau and the archipelago were emplaced during Tertiary time (40–45 Ma), as the volcanic output rate reduced. Furthermore, intraplate volcanism continued in the Kerguelen archipelago for at least 40 Ma. The isostatic compensation of the Kerguelen Isles and the Kerguelen–Heard Plateau is achieved by low-density mantle material, as shown by refraction and geoid studies.

The velocity–depth structure below the Kerguelen Isles is similar to that found below intraplate oceanic islands such as Hawaii. Despite the differences in age, the crust below Iceland (0 Ma) and the Kerguelen Plateau (100–120 Ma) are strikingly akin. The similarity between the Kerguelen–Heard Plateau and Iceland, then, strongly supports a similar origin for both structures, the Kerguelen–Heard Plateau being a fossil equivalent of present-day Iceland.

Crustal thickening beneath the Kerguelen–Heard Plateau, which may result from an Iceland-type setting (i.e. an active spreading centre over a hotspot), is mostly produced by thickening of layer 3, layer 2 representing 25 per cent only of the thickness of the igneous crust. The Kerguelen Isles, despite the initial volcanism near the active Southeast Indian Ridge, behave as a midplate volcanic island and are definitely not representative of the whole Kerguelen Plateau structure.

Key words: hotspot, Kerguelen, lower crust, oceanic islands, oceanic plateau, underplating.

INTRODUCTION

The Kerguelen Isles (Terres Australes et Antarctiques Françaises, TAAF) and the Australian Heard and MacDonald Islands, located 500 km south of the Kerguelen Isles (Figs 1 and 2), are the sole subaerial fragments of the Kerguelen Plateau stretching from 46°S to 64°S in a NNW–SSE direction with an average breadth of 450 km.

At the turn of the century, pioneering exploratory voyages of the British ship HMS *Challenger,* and the German ships SMS *Valdivia* and *Gauss* led early authors (Murray & Renard 1885; Chun 1903; von Drygalski 1912) to portray these islands as subaerial fragments of one large submarine feature running from north of the Kerguelen Isles towards Antarctica. The province of the northern Kerguelen Plateau stretching from 46°S to 55°S is labelled the Kerguelen–Heard Plateau (Figs 1 and 2). The main island of the Kerguelen Isles has a somewhat triangular shape and is roughly 130 km long and 120 km across (Figs 2 and 3). The Kerguelen Isles consist mostly of Hawaiian-type flood basalt coating 85 per cent of the surface (Aubert de la Rüe 1932; Mawson 1934; Nougier 1970; Giret 1983). Some stratovolcanoes break through the thick series of flow basalts. Mont Ross, culminating at 1850 m, is the most prominent feature of the Kerguelen Isles (Fig. 3). Volcanism has been active from 40 Ma to the present on Kerguelen and Heard Islands. The last eruptions occurred in the archipelago a few thousand years ago (Giret 1983). Eruptions from the 2800 m-high Big Ben on Heard Island (Fig. 2) have been witnessed by early sailors, and recently from M/V *Marion Dufresne* (TAAF) in 1985 and 1993. Plutonic ring complexes of miscellaneous types are numerous in the Kerguelen Isles; the largest one (Figs 2 and 3) lies in the westerly Rallier du Baty Peninsula (Aubert de la Rüe 1932; Nougier 1970;

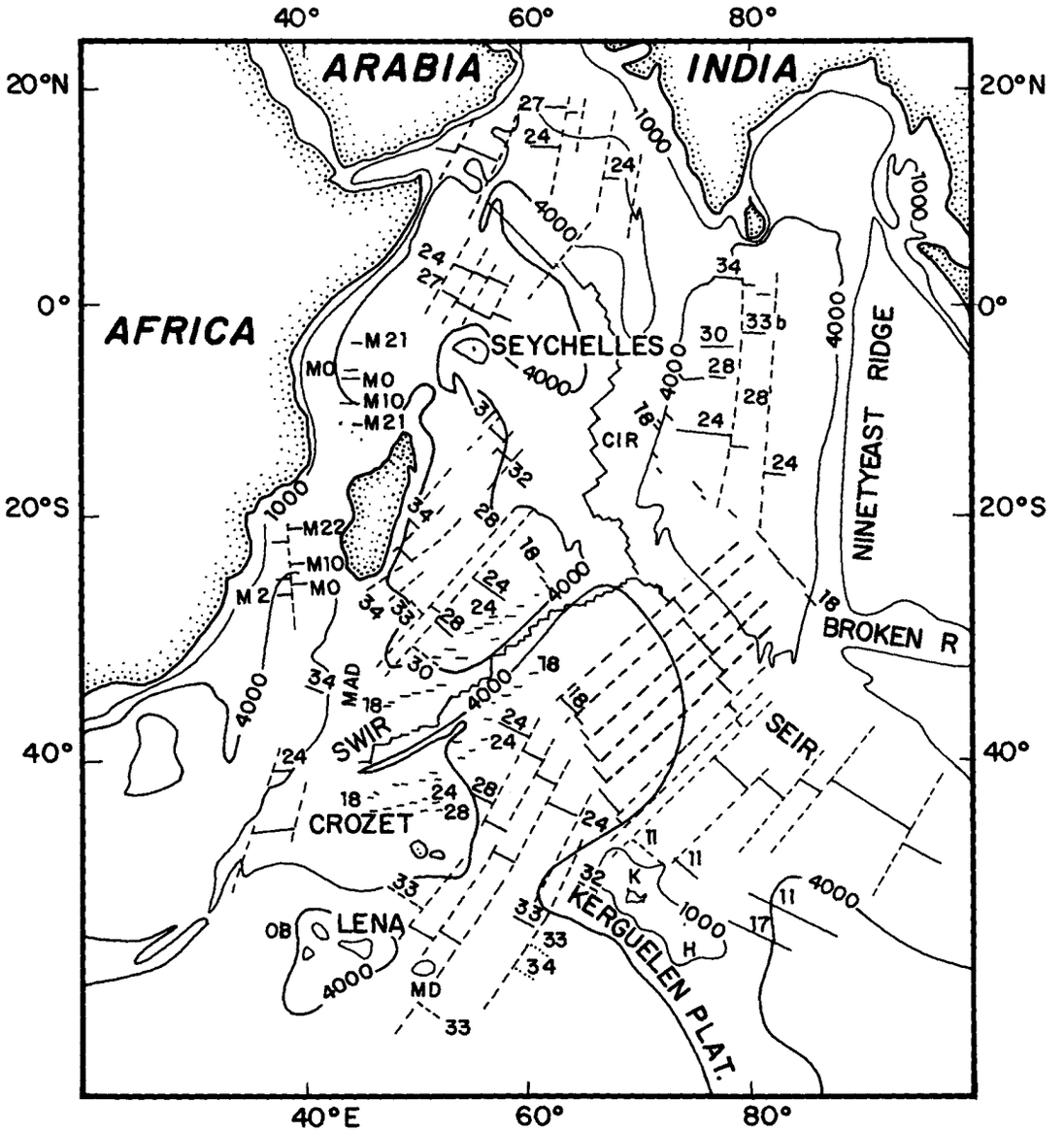

Figure 1. Bathymetric contours in metres, major physiography, magnetic anomaly identifications and fractures zones of the SW Indian Ocean after Schlich (1983) and Goslin & Patriat (1984). CIR: Central Indian Ridge; SEIR: SE Indian Ridge; SWIR: SW Indian Ridge. MD and OB: Marion Dufresne and Ob seamounts; K: Kerguelen; H: Heard islands.

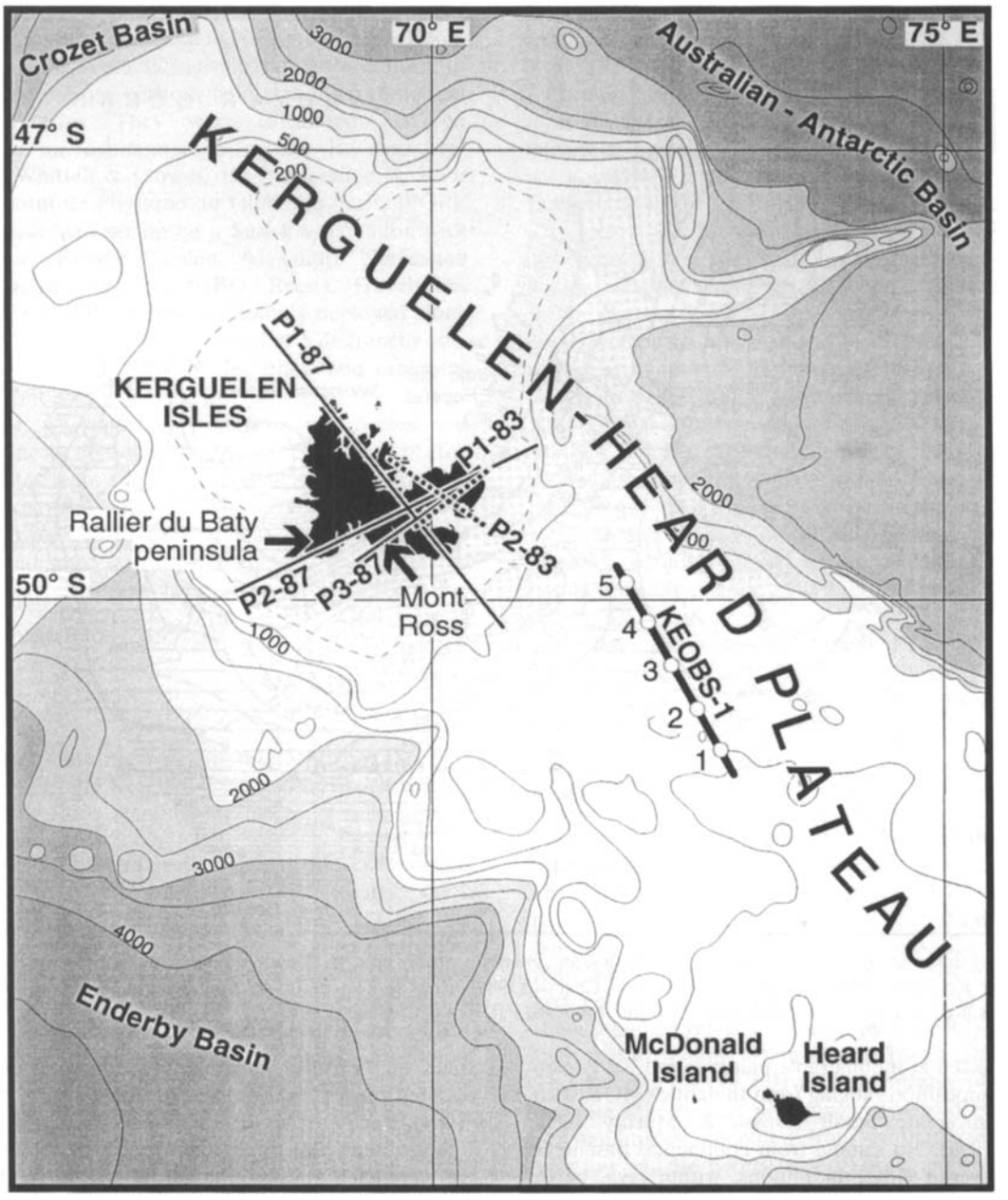

Figure 2. Bathymetric map of the northern Kerguelen Plateau. Depths are in metres with a contour interval of 500 m. Bathymetry is from Houtz *et al.* (1977) and Schlich *et al.* (1987). Field seismic lines across the Kerguelen Isles, shots being fired at sea in 1983 and 1987, and profile KeOBS1, south of the Kerguelen Isles, are plotted. OBSs are marked by open circles on KeOBS1, from OBS 1 at the southern end of the profile northward to OBS 5.

Lameyre *et al.* 1976, 1981; Giret 1980, 1983; Giret & Lameyre 1983), where severe enduring glacial erosion has exposed, in addition to the lavas, a series of plutonic rocks: syenite, monzonites, diorites and gabbros (Edwards 1938). At least six glaciers on the west and south descend practically to sea-level; the most important one, Glacier Cook, caps the centre of the main island (Fig. 3).

The subdued Kerguelen–Heard Plateau is affected by steep faulting (Fig. 2). The water depth is between 0.50 km and 0.75 km over most of the plateau. Bounding slopes are steeper in the east (5°–10°) than in the west (1°–3°) and are commonly disrupted by peaks and ridges. High-amplitude and short-wavelength magnetic anomalies denote at first glance a basaltic basement (Schlich 1975; Goslin 1981; Schaming & Rotstein 1990).

Refraction data related to the deep crustal structure of the Kerguelen Isles have been collected (Fig. 2) by ourselves (Recq, Charvis & Hirn 1983; Charvis 1984; Recq & Charvis 1986; Recq *et al.* 1990; Recq 1991; Recq *et al.* 1994) throughout the south-eastern region of the archipelago in 1983 (profiles P1-83 and P2-83), and across the archipelago in 1987 (profiles P1-87, P2-87 and P3-87). Data were collected at sea on the northern (Fig. 2) and southern domains of the Kerguelen Plateau (MD66/KeOBS cruise) along refraction lines carried out in 1991 (Charvis, Operto & Recq 1992; Charvis *et al.* 1993; Operto 1995).

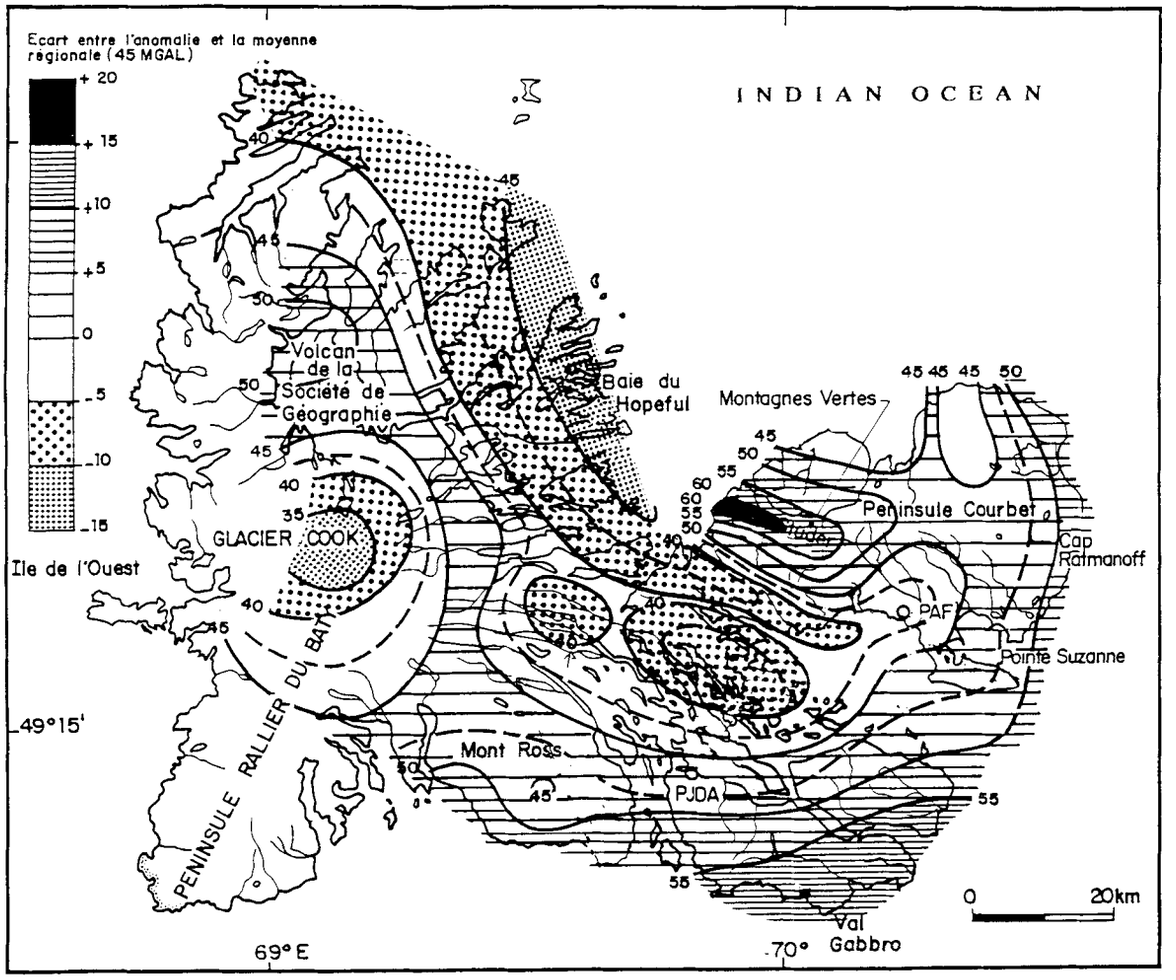

Figure 3. Some of the general features of the Kerguelen Isles, and gravity contours relative to the regional mean value of the Bouguer anomaly (+45 mgal), after Rouillon (1963); previously published in Charvis (1984), Recq & Charvis (1986) and Recq *et al.* (1990). Profile P2-83 was reversed by shots fired in Baie du Hopeful. PAF: Port-aux-Français, PJDA: Port-Jeanne d'Arc.

Samples collected at innumerable places in the Kerguelen Isles show a composition ranging from tholeiitic (MORB) to alkaline-type intraplate basalt (Dosso & Murthy 1980; Gautier *et al.* 1990). No sample from continental basement has been discovered either in plutons, within lava, or in ejecta, on either Kerguelen or Heard Islands (Chun 1903; von Drygalski 1912; Stephenson 1964; Watkins *et al.* 1974; Marot & Zimine 1981; Gautier *et al.* 1990), or in samples from ODP Leg 120 boreholes on the Kerguelen Plateau (Rotstein *et al.* 1990; Munschy *et al.* 1992). Nevertheless, Ramsay *et al.* (1986) and Montigny, Karpoff & Hofmann (1993) reported that granitic debris (ice rafted?) was dredged in the southern Kerguelen Plateau. From refraction studies, Operto & Charvis (1995) and Operto (1995) do not preclude continental fragments within the southern domain. Early investigations showed that Broken Ridge and the Kerguelen–Heard Plateau were built up by melt generated by adiabatic decompression in the vicinity of the Southeast Indian Ridge (Le Pichon & Heirtzler 1968; McKenzie & Sclater 1971; Goslin, Recq & Schlich 1981).

Interpretation of refraction lines running throughout the archipelago (Recq *et al.* 1983; Charvis 1984; Recq & Charvis 1986; Recq *et al.* 1990; Recq 1991; Recq *et al.* 1994) suggests that a continental origin for the Kerguelen Isles has to be ruled out. Further information on these experiments and detailed results are reported by Recq *et al.* (1983), Charvis (1984), Recq & Charvis (1986), and Recq *et al.* (1990).

Seven refraction lines were shot at sea in early 1991 on the Kerguelen Plateau and nearby. MD66/KeOBS cruise on M/V *Marion Dufresne* (TAAF) was conducted by ORSTOM (Office de la Recherche Scientifique et Technique Outre-Mer, now Institut Français de Recherche Scientifique pour le Développement en Coopération) and the then Mission de Recherche des TAAF (now Institut Français pour la Recherche et la Technologie Polaires, IFRTP, Brest) with the collaboration of the Université de Bretagne Occidentale at Brest (UBO, Unité de Recherche Associée 1278 du CNRS).

At sea, five three-component digital OBSs were distributed evenly on each 130–180 km long profile. These OBSs were designed by the Institute for Geophysics of the University of Texas at Austin (Nakamura *et al.* 1987) and operated by the ORSTOM branch at Villefranche-sur-mer. The seismic source consisted of an untuned array of eight 16 l air guns provided and run at sea by GENAVIR/IFREMER (Brest), resulting in a shot spacing of approximately 200 m. GPS provided continuous ship positions. The location of OBSs on the sea-bottom relative

to the ship was computed using traveltime and polarity of the direct water wave as discussed in Nakamura *et al.* (1987).

Ray tracings and synthetic seismograms were used to model observations from onshore field stations installed on the Kerguelen Isles. They were calculated first on IBM-compatible microcomputers using the Rayamp program (Spence, Whittall & Clowes, 1984) upgraded by Raul Madariaga (Institut de Physique du Globe de Paris, IPGP). This program was then set up on a Sun 4 workstation with the assistance of Roland Gaulon, Alexandre Nercessian (IPGP) and Daniel Aslanian (UBO, Brest). Traveltimes from the whole set of five OBSs successfully deployed along profile KeOBS1 (Fig. 2) were processed at Villefranche-sur-mer on Sun 4 using the Rayinvr algorithms and programs developed by Zelt & Smith (1992).

In this paper, we report and interpret unexpected and striking differences between the crustal structure of the Kerguelen archipelago and the Kerguelen–Heard Plateau revealed by explosive refraction lines running throughout the archipelago with shots fired at sea, and by the profile KeOBS1 carried out on the Kerguelen–Heard Plateau between the archipelago and Heard Island (Fig. 2).

RESULTS

The Kerguelen Isles

We discuss briefly the main results inferred from the 1983 and 1987 surveys in the Kerguelen Isles (Charvis 1984; Recq & Charvis 1986; Recq *et al.* 1990). Some seismic profiles have been reprocessed.

On ray tracings, each ray group is labelled GR*x* according to the refracting layers and related boundaries: GR1, shallow structure; GR2, layer 2; GR3, layer 3; GR4, the crust to mantle transition zone; GR5, *Pn* wave refracted within the upper mantle; GR6, reflected waves from layer 2/layer 3 boundary; GR7, reflected waves from the base of layer 3 at the top of the crust–mantle transition zone; GR8, *PmP*, Moho reflections. At sea, a mean velocity of 3.20 km s^{-1} was ascribed to the shallow marine Pliocene–Quaternary layer (Houtz, Hayes & Markl 1977; Li 1988). From short-range onshore experiments (test shots), a seismic velocity ranging from 3.80 to 4.17 km s^{-1} was calculated for the shallow basaltic piles of the Kerguelen archipelago (Charvis 1984; Recq & Charvis 1986).

Profile P2-83 (Fig. 4)

This profile running through Val Studer at the western boundary of Péninsule Courbet (Figs 2 and 3) is properly reversed by shots (explosive) fired at either end. P2-83 has been reinterpreted introducing a crust to mantle transition zone (see the P2-87 profile and the section devoted to the crust–mantle boundary), as postulated earlier by Recq *et al.* (1990), and a dipping Moho. In the upper crust, velocities of 4.60–4.90 km s^{-1} (GR2) increasing with depth to 5.60–6.00 km s^{-1} are within the range of velocities in oceanic layer 2. The basalt thickness below this profile, which skirts the western boundary of Péninsule Courbet, ranges from 9 to 8 km north-westwards, i.e. far greater than that encountered below deep oceanic basins (Recq 1983; White, McKenzie & O'Nions 1992). The lower crust is about 6–7 km thick with velocities ranging downwards from 6.75 to 6.80 km s^{-1}. These values fall within the range of oceanic layer 3 velocities. Furthermore, velocities of about 7.95 km s^{-1} were observed on this profile as first arrivals at short distances, beyond 45 km (Fig. 4a, GR5). The crustal thickness, including the transition zone, slightly decreases north-westwards and below Val Studer (Fig. 4b), from 17 km to 15 km at the northernmost end of this profile.

At a first step in the interpretation of profile P2-83, the nearby Montagnes Vertes plutonic complex might produce higher velocities within the upper crust than those observed within plateau basalt. The reversed profile (Fig. 4b), shots being fired at the northern end of P2-83, leads us to discount this latter hypothesis. Computed traveltimes at short ranges on the reversed profile mismatch the observed traveltimes. Although P2-83 crosses the Montagnes Vertes plutonic ring complex (Fig. 3), this intrusive feature has a poor horizontal extent, as shown from gravity data. The short-wavelength positive gravity anomaly (Fig. 3) in this region (Rouillon 1963; Charvis 1984) rules out a deep origin, but denotes the presence of high-density material intruding this plateau basalt at shallow depth, with a seismic velocity ranging from 4.85 to 6.00 km s^{-1}.

We note that at the end of profile P1-83 (Fig. 2), *Pn* waves have been recorded as first arrivals beyond 50 km, but the data are scarce and the interpretation disputable (Recq *et al.* 1983; Charvis 1984; Recq & Charvis 1986).

Profile P1-87 (Fig. 5)

This profile runs across the Kerguelen archipelago from the south-east to the northernmost part of the main island. Shots were fired at sea at either end of P1-87. The seismic record section of the northernmost shot of profile 1 (Fig. 5b) does not exhibit any upper crustal velocities as first arrivals. However, shots fired at smaller distances from the archipelago, on the same northern section of this profile, show a higher velocity within layer 2 (GR2) of 5.50 km s^{-1}, than that prevailing within plateau basalt (Recq *et al.* 1990). This velocity may be related to a volcanic plutonic complex piercing the crust as previously suspected by Giret (1983). *Pn* amplitudes computed from synthetic seismograms are very low and are poorly (or not) observed on record sections (GR5). However, there is a quite good correlation on record sections between reflected waves and observed high-amplitude phases. The average depth of the crust below P1-87 is 19 km.

Profile P2-87 (Fig. 6)

Some seismic data collected on profile P2-87 running through the archipelago (SW–NE trending) have been reprocessed. To match computed traveltimes to observed ones, higher velocities (GR1, 5.75 to 6.20 km s^{-1}) at shallow depths than those ascribed to basalt layers are indicated at the south-western Kerguelen archipelago. These high velocities are probably related to the Rallier du Baty plutonic ring complex (Figs 2 and 3). At the intersection of this profile with P2-83, the structure of the upper crust computed from P2-87 is roughly compatible with that modelled from profile P2-83, the basalt layers being 9.5 km and 9 km thick respectively. The thickness of the crust is

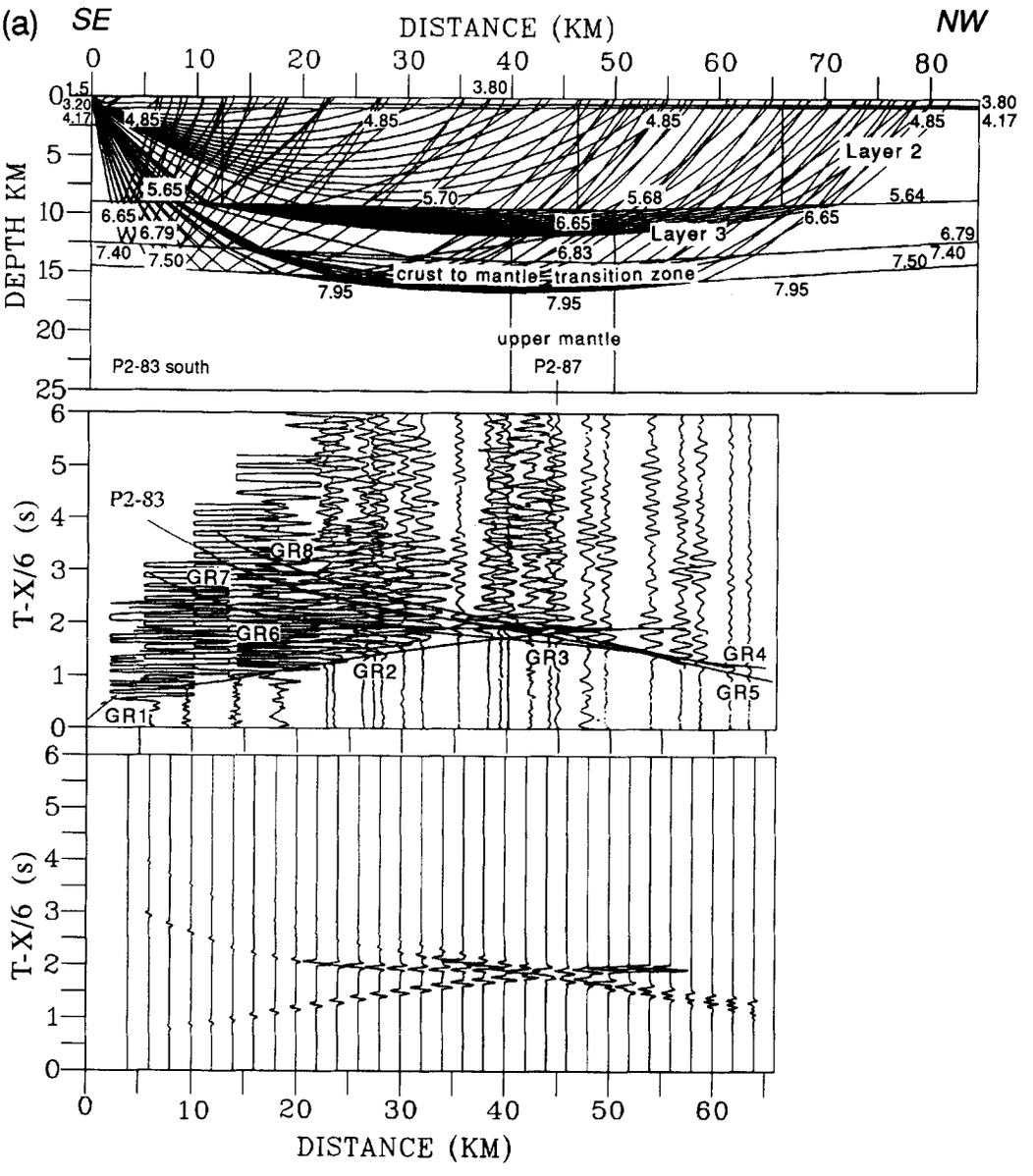

Figure 4. For more clarity, only one out of two rays has been plotted in Figs 4–6. Record section, ray tracing, synthetic seismograms and crustal structure below the reversed profile P2-83 (Fig. 2). The reduced velocity is 6 km s^{-1}. (a) Shots fired at the southern end of the profile; (b) shots fired in the Baie du Hopeful (Fig. 3), at the northern end of the profile. The Moho depth is shallower (15–17 km) than below the central region of the archipelago. The crust thins oceanwards below the Péninsule Courbet.

roughly the same, 18–19 km, on both profiles. Excluding the central Kerguelen Isles, velocities within basalts (GR2) are comparable to those observed on P2-83. Within the lower crust, velocities are quite similar on both profiles. For the lower crust and upper mantle, several aspects of both experiments (1983 and 1987) appeared to be in conflict (Charvis 1984; Recq & Charvis 1986; Recq *et al.* 1990). A closer examination of the forward and reversed composite profiles P2-87 exhibited very low, and perhaps dubious, amplitudes of *Pn* as first arrivals (GR 5, Figs 6a and b) at distances beyond 100–110 km either side of the profile. Modelling the transition to mantle zone (GR4, Fig. 6b) shows that the velocity within this feature is about 7.4 km s^{-1} to 7.6 km s^{-1}. A small velocity contrast and/or a low velocity gradient within the upper mantle may cause very low amplitudes of waves refracted in the upper mantle (GR5, Figs 6a and b). Inspection of waves refracted within the transition zone (GR4) and reflected waves (GR6, GR7 and GR8) shows that the crust thins north-westwards from 17 to 15–16 km towards the northern Kerguelen Plateau.

Some remarks on the crust–mantle boundary below the Kerguelen Isles

Profile P2-83 largely differs from P1-87 and P2-87. *Pn* waves are recorded on profile P2-83 as first arrivals at very short ranges. On P1-87 and P2-87, *Pn* waves are often dubious and when they are observed, their amplitudes are very low. This suggests a very low velocity gradient within the upper mantle. Synthetic seismograms enable us to remove the

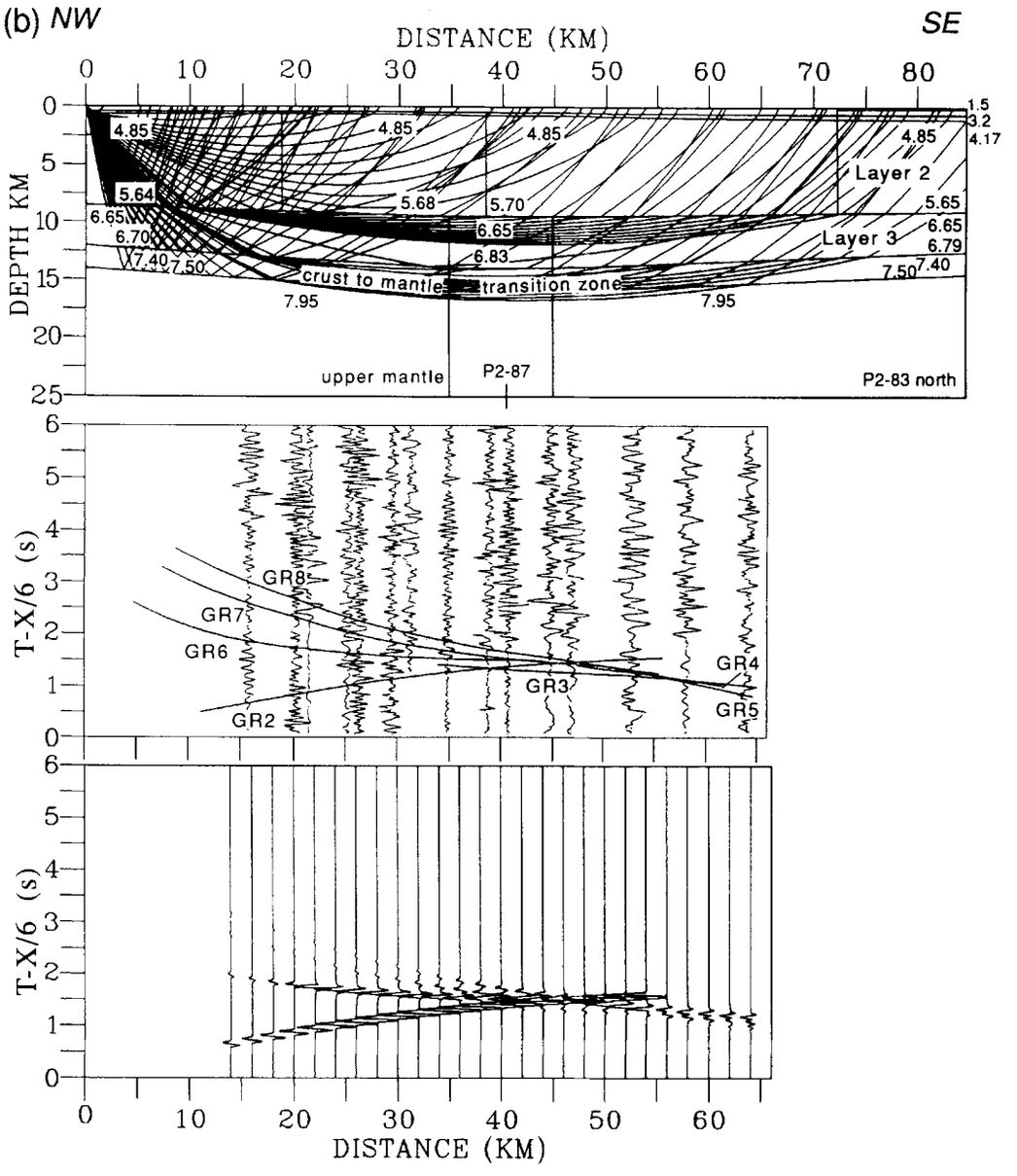

Figure 4. (*Continued.*)

apparent contradiction between the 1983 and 1987 results. The transition to mantle velocities at the base of the crust (GR4, Figs 4–6) lead to high-amplitude upward-refracted waves travelling at a velocity of 7.4–7.5 km s^{-1} (Fig. 4b). In Fig. 4(a), rather high amplitudes (GR4) are sharply discontinued at short ranges, showing that at about a depth of 19–20 km a drop of velocity gradient associated with a possible low-velocity mantle may cause the sharp decrease of amplitude. In Fig. 4(b), phase GR4 is observed at greater distance, indicating either a deeper crust–mantle interface or a lower velocity gradient within the transition to mantle at the northern end of P2-87 (Péninsule Galliéni, Figs 2, 6a and 6b). The velocity gradient within the upper mantle being low, amplitudes of *Pn* waves drop dramatically to very low values, as seen in Figs 4, 5 and 6. The observation of high-amplitude seismic waves travelling through a rather high-velocity gradient zone shortly followed by low-amplitude waves suggests the possible occurrence of a crust–mantle transition zone over a low-velocity-gradient upper mantle and even with a slight downward decrease of velocity within the upper mantle below the Kerguelen Isles. Moreover, negative velocity gradients within the upper mantle below a variety of features have already been reported in earlier works (Bowin 1973; Dziewonski & Anderson 1981; Souriau 1981; Lewis 1983; Whitmarsh, Avedik & Saunders 1986).

The amplitude of *Pn* waves being rather low on P1-87 and P2-87, the interpretation of phases interpreted as refracted waves within the transition zone (GR4, Fig. 6b), waves reflected from the top of the transition to the mantle layer (GR7) and waves reflected from the Moho (PmP, GR8) provides us with a rather good estimate of the crustal thickness of the archipelago. Fig. 6(b) (P2-87) shows that beyond 80 km GR8 and GR4 arrive close together. The

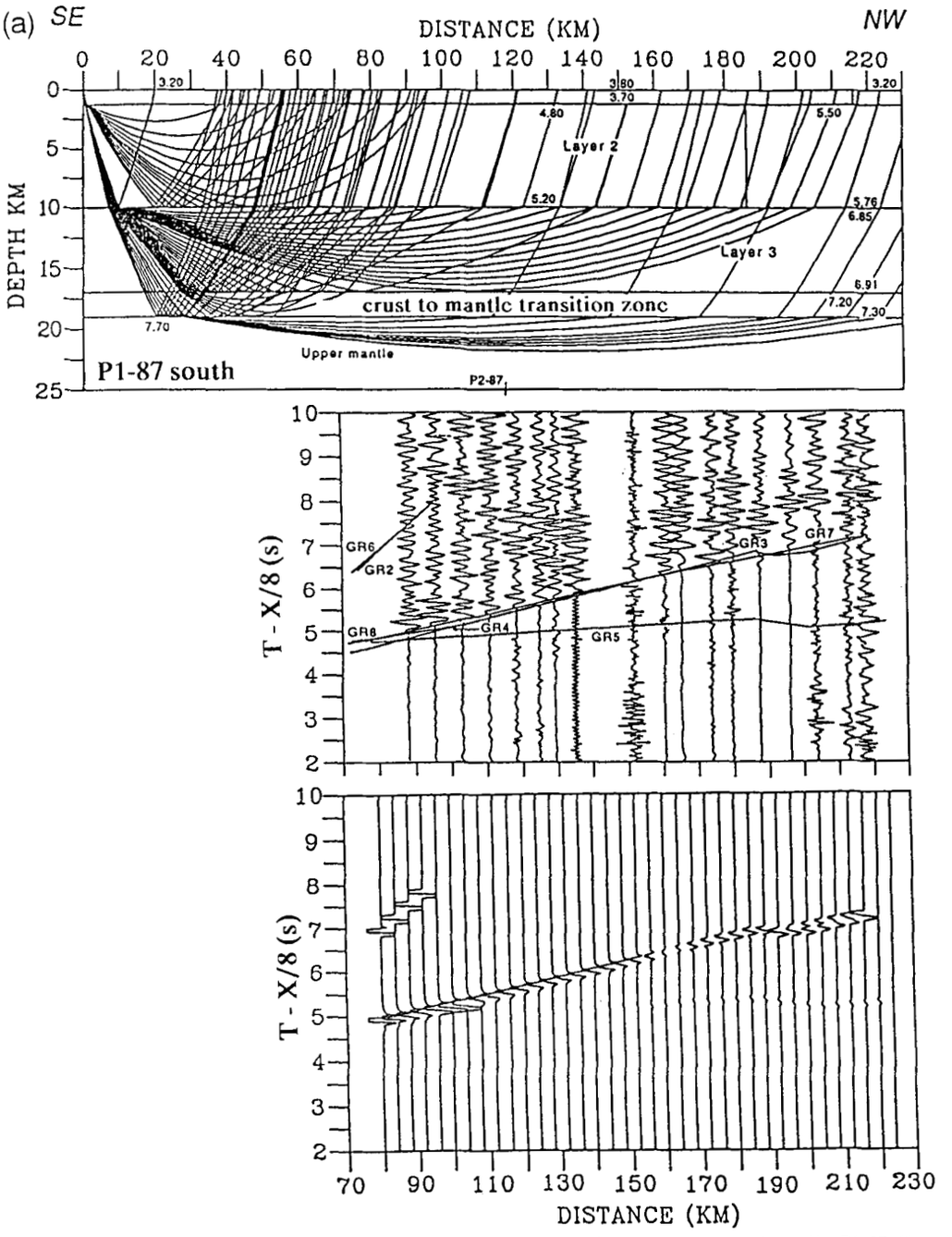

Figure 5. Record section, ray tracing, synthetic seismograms and crustal structure below the reversed profile P1-87 (Fig. 2). The reduced velocity is 8 km s^{-1}. (a) Shots were fired at the southern end of the profile; (b) shots were fired at sea, north of the archipelago. High amplitudes (GR3) on synthetic seismograms beyond 190 km denote the sharp increase in velocity from 4.80 km s^{-1} to 5.50 km s^{-1}, presumably related to the Volcan de la Société de Géographie plutonic complex (Fig. 3).

accord between depths of interfaces at the intersection of profiles is rather good between P1-87 and P2-87 (±1 km), attesting to the simplicity of crustal models. *Pn* waves being dubious below P2-87, the accord deteriorates between P2-83 and P2-87 (Figs 4 and 6). At the southern end of profile P1-87, the farthest shot south of the Kerguelen Isles has been fired at 70 km from the archipelago. We do not know whether the crustal structure below this shot is related to the Kerguelen Isles or to the Kerguelen–Heard Plateau, and this causes an additional uncertainty in the actual Moho depth below the archipelago.

The Moho reaches a depth of 19–20 km in the very central region of the main island. North-eastwards towards the ocean, the crust thins rapidly to only 16 km.

The Kerguelen–Heard Plateau

Five OBSs evenly distributed along the 150 km long KeOBS1 profile (Fig. 2) were deployed successfully along the line to model the crustal velocity structure below the Kerguelen–Heard Plateau. A preliminary interpretation of

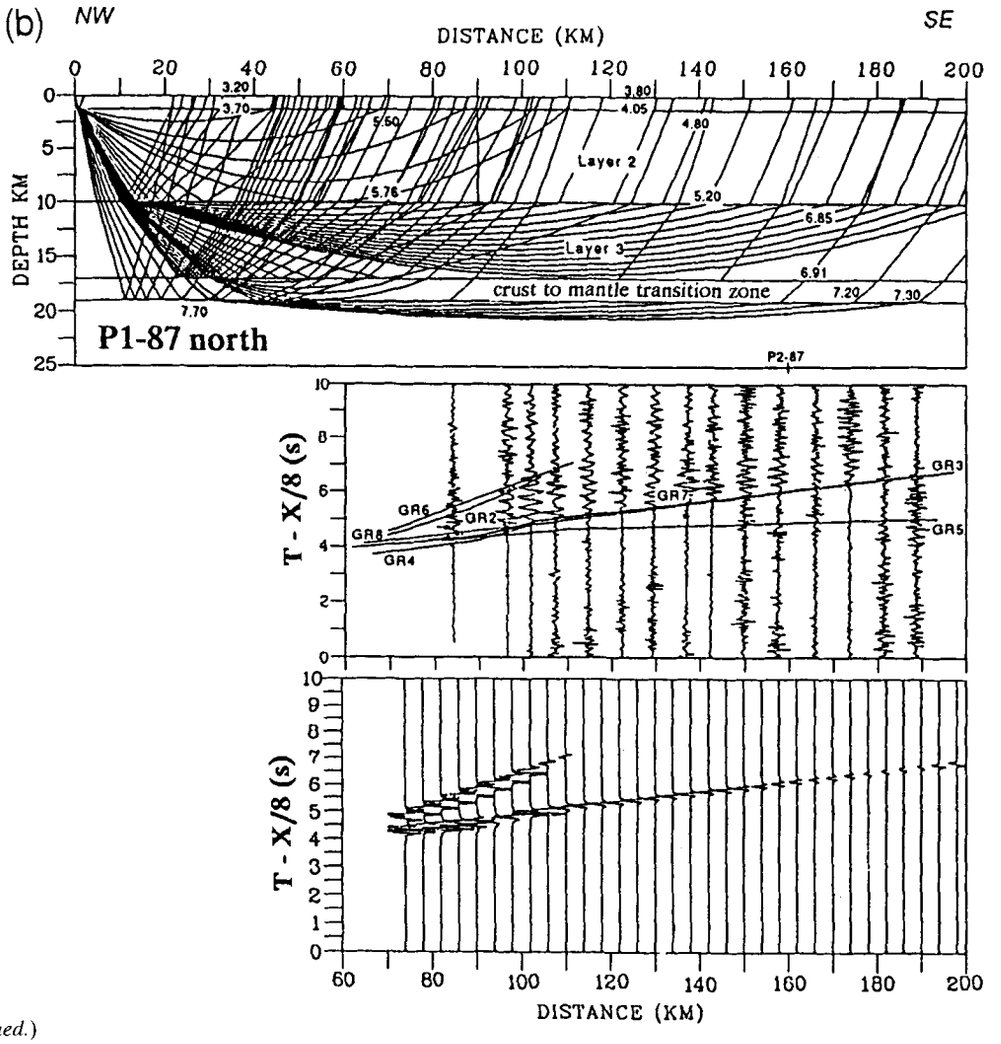

Figure 5. (*Continued.*)

this line based upon standard ray tracing only was previously published by Charvis *et al.* (1993). Nevertheless, the high density of the available data makes detailed crustal modelling rather difficult to conduct using trial-and-error forward modelling programmes. A total of 750 shots were fired (on average 200 m apart) and recorded simultaneously along this line by the whole set of OBSs. For a far more detailed interpretation, traveltimes from all OBSs were inverted simultaneously using the 2-D inversion routine of Zelt & Smith (1992).

The five record sections do not exhibit notable differences (Figs 7a–e). Table 1 summarizes seismic waves identified on record sections and then used for inversion. Seismic waves refracted in the sedimentary cover (c.1) are observed at distances less than 10 km always as second arrivals (Figs 7a–e). Seismic phase (d.1) could be related either to refraction in the sedimentary cover or in the basement (Figs 7a–e). Seismic wave (e.1) refracted within the basement (Figs 7a–e) exhibits a strong curvature, suggesting a sharp downward velocity increase (high velocity gradient), whereas (f.1) refracted in the deeper crust is quasi-linear (Figs 7a–e) within the range from 25 to 125 km, implying a low velocity gradient and a thick layer. Arrivals of upgoing rays reflected from deep reflectors are visible on all OBS sections (Figs 7a–e). The reflection observed on OBSs 3 and 5, labelled (f.2) in Figs 7(c) and (e), is modelled as a *PmP* wave (reflection from the Moho), whereas those observed on OBSs 1 and 2 (Figs 7a and b) and labelled (h) could be related to upgoing rays reflected from deeper interfaces within the upper mantle. This latter phase is beyond the scope of this paper. No refracted waves from beneath the crust–mantle boundary (*Pn*) are identifiable as first arrivals on any of these seismic sections (Figs 7a–e). However, a low-amplitude linear phase (g.1′) is observed from 100 to 135 km on the OBS 5 record section (Figs 7e and 8) between *PmP* (f.2) and the multiple of *PmP*. This latter is reflected downwards from the top of the water column (Fig. 8). The apparent velocity of 8.3 km s^{-1} or so and traveltimes of (g.1′) with respect to the *PmP* multiple suggest that (g.1′) could be the multiple of the *Pn* wave. At distances over 70 km on the OBS 5 section (Fig. 7e), amplitudes of multiples are slightly greater than amplitudes of direct waves. This accounts for the observation of multiples of *Pn* even though the direct *Pn* wave is not observed (or ill-observed).

The identification of the main refracted and reflected waves observed on all seismic sections allows us to construct an initial seven-layer model of the crust below the Kerguelen–Heard Plateau. This model is defined by depths of interfaces and velocities at the top and the bottom of each

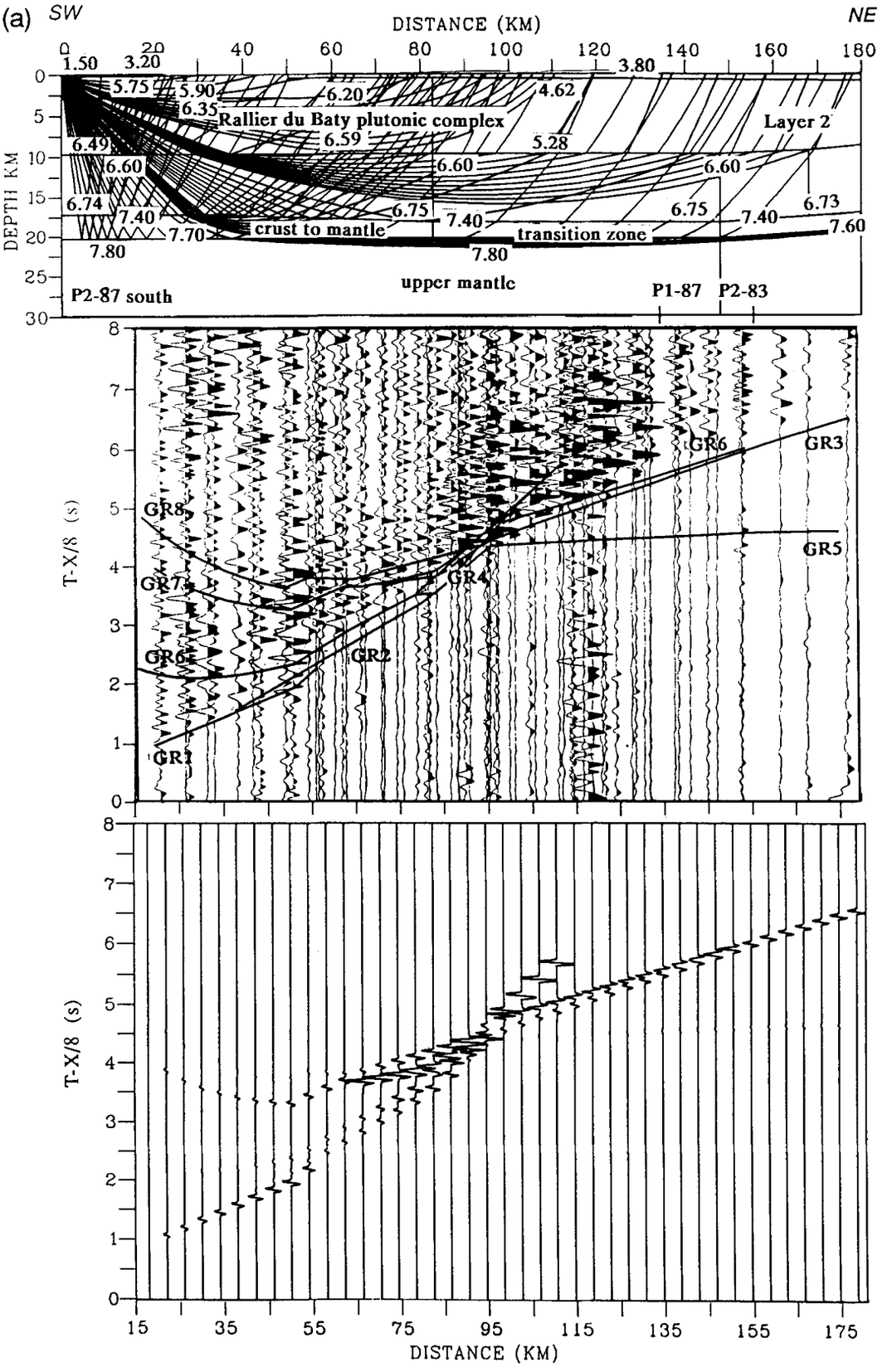

Figure 6. Ray tracing, reprocessed record section, synthetic seismograms and crustal structure below composite profile P2-87 shot off (a) the Rallier du Baty plutonic complex, and (b) Péninsule Courbet, at the south-western and the north-western ends of the profile, respectively. The reduction velocity is 8 km s^{-1}. This crustal model differs slightly from that previously published in Recq *et al.* (1990). *Pn* waves are poorly developed (GR5).

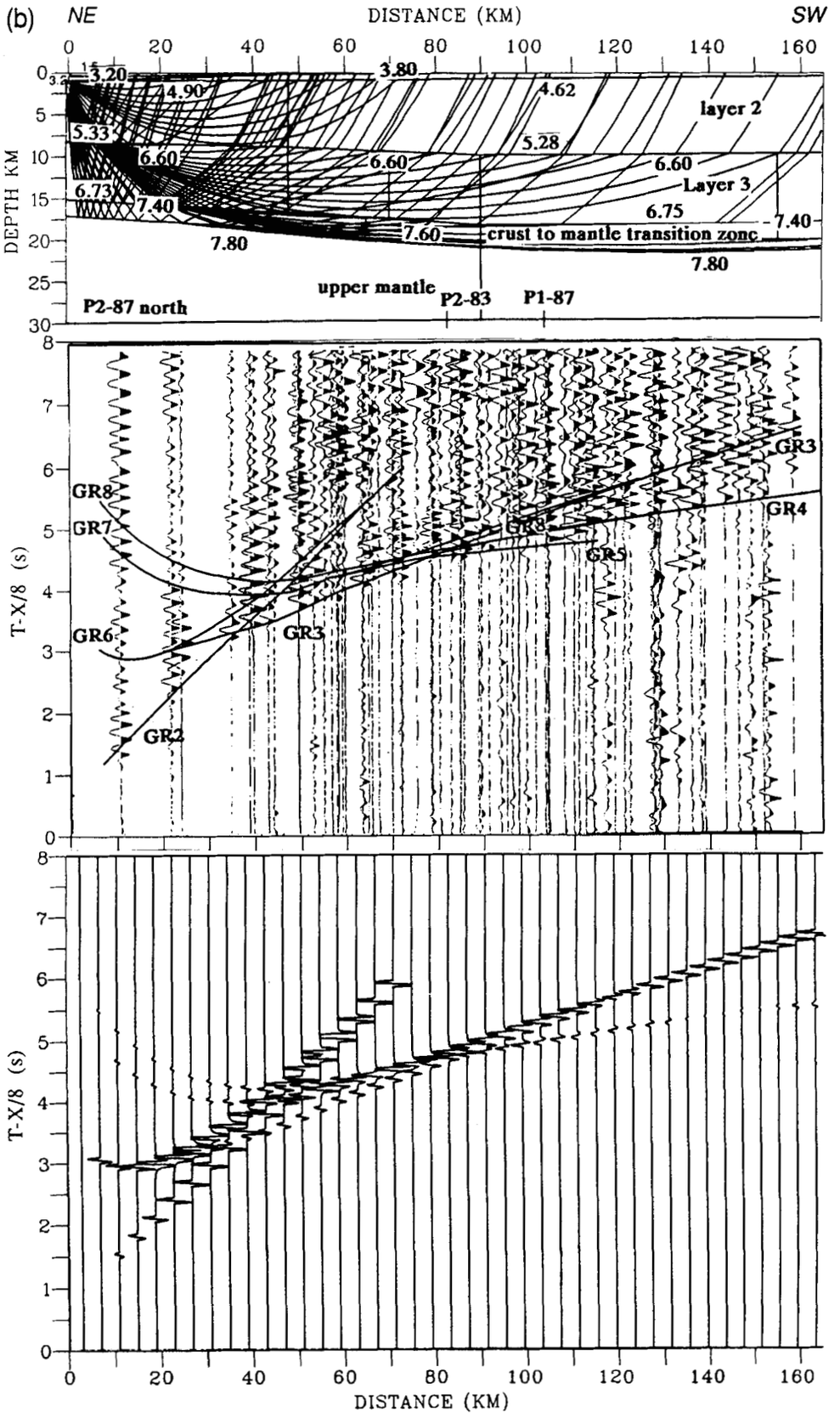

Figure 6. (*Continued.*)

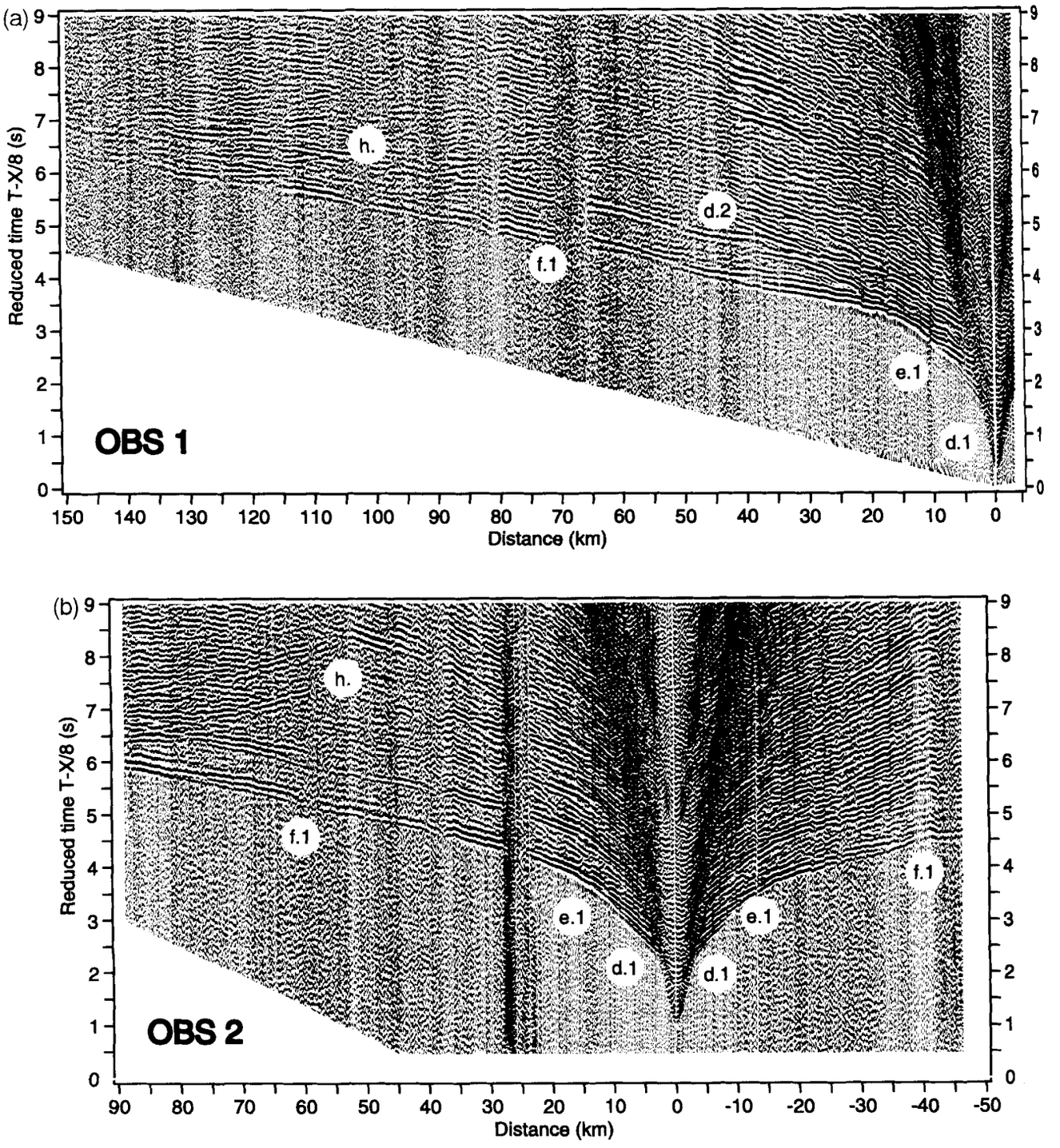

Figure 7. Seismic sections recorded by each of the five OBSs deployed along profile KeOBS1. A gain proportional to the distance is applied to the data. Nevertheless, large amplitudes are clipped. Data are bandpass filtered by applying a 5–20 Hz Butterworth filter, except the data from OBS 5 which are bandpass filtered with a 8–20 Hz Butterworth filter. The reduction velocity is 8 km s $^{-1}$. Arrivals are labelled from (c.1) to (h) as shown in Table 1.

layer (interface and velocity nodes). The number of interfaces and velocity nodes is defined by the user to optimize 'stopping' criteria (Table 2). The inversion of seismic data was applied iteratively as described by Zelt & Smith (1992). Layers are labelled A to G downwards from the top. The thickness of layer A, the water layer, is computed from the shipborne 12 kHz wide-beam echo-sounder. The water velocity, 1.46 km s^{-1}, is extracted from Carter's area 33 (Carter 1980). Layer B is the uppermost sedimentary layer not directly observed from refraction data, but inferred from the traveltimes and intercepts of *P* waves refracted within layer C (Charvis *et al.* 1993). The velocity in layer B, 1.65–1.71 km s^{-1}, was computed from sonobuoy refraction data by Munschy & Schlich (1987).

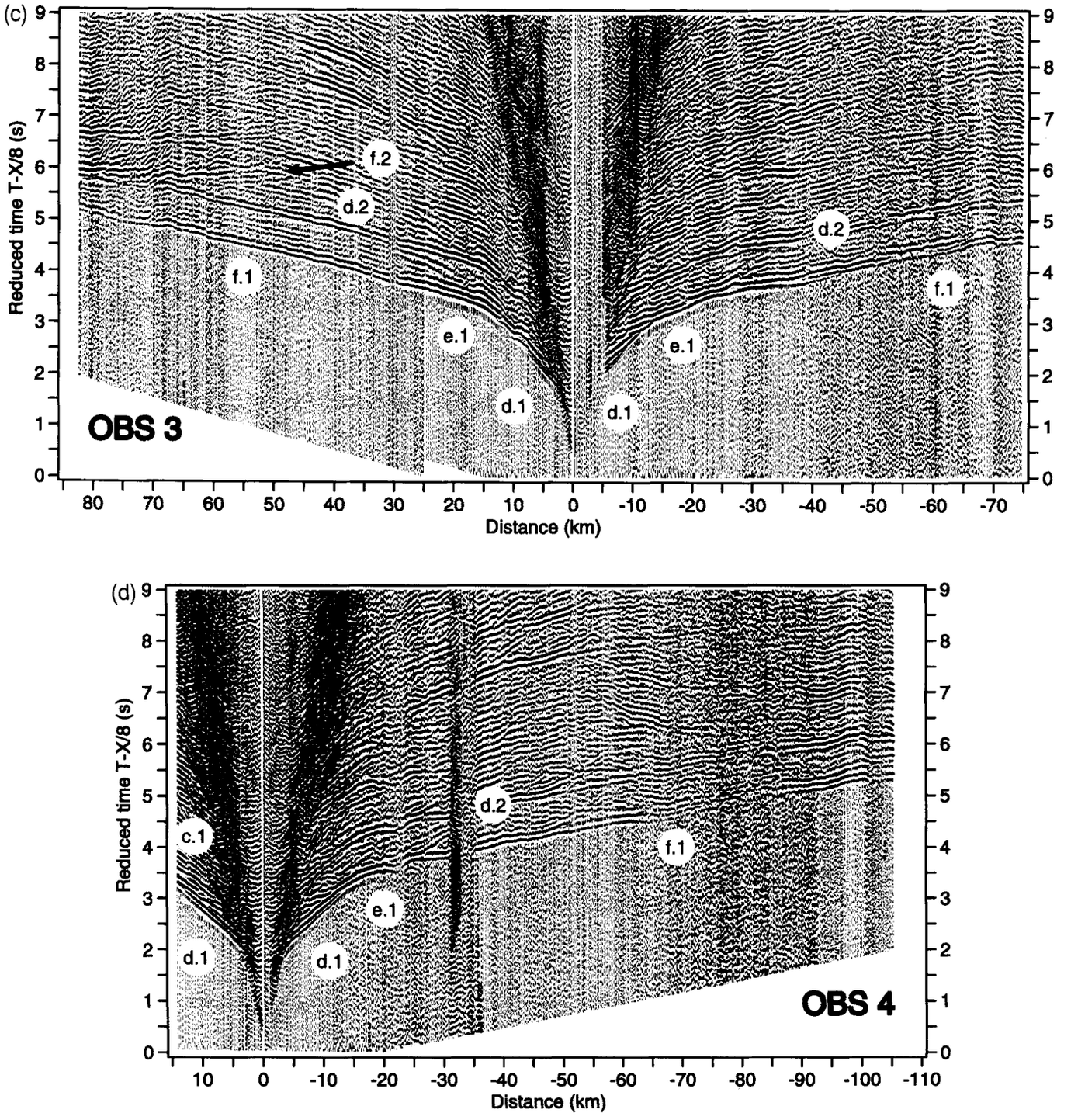

Figure 7. (*Continued.*)

The ray coverage is excellent down to a depth of 23 km (Fig. 9). Criteria used to test the fit between observed and computed traveltimes are the root-mean-square traveltime residual T_{rms} and χ^2. We assumed that the fit was acceptable as $T_{rms} \leq 0.1$ s and $\lambda^2 \leq 1.0$ (Zelt & Smith 1992). All phases, except the reflection from the top of layer F (wave code d.2; see Table 2 and Figs 7a, c, d and e), meet the criteria. Resolution values, according to the definition of Zelt & Smith (1992), indicate relative ray coverages at a specified node. Node points with resolution values ≥ 0.5 are considered to be well resolved. Resolution values for velocities in the final model are always higher than 0.75, except at the edges of the model where the ray path coverage is scarce (Figs 9 and 10). Resolution values for depths of interfaces are always higher than 0.75.

Figure 11 shows that the 1.0–1.8 km thick sedimentary cover is split into two distinct layers B and C. The upper one, layer B, has velocities ranging from 1.65 to 1.71 km s^{-1}, as reported by Munschy & Schlich (1987), and reaches a maximum thickness of about 1.0 km, whereas the lower

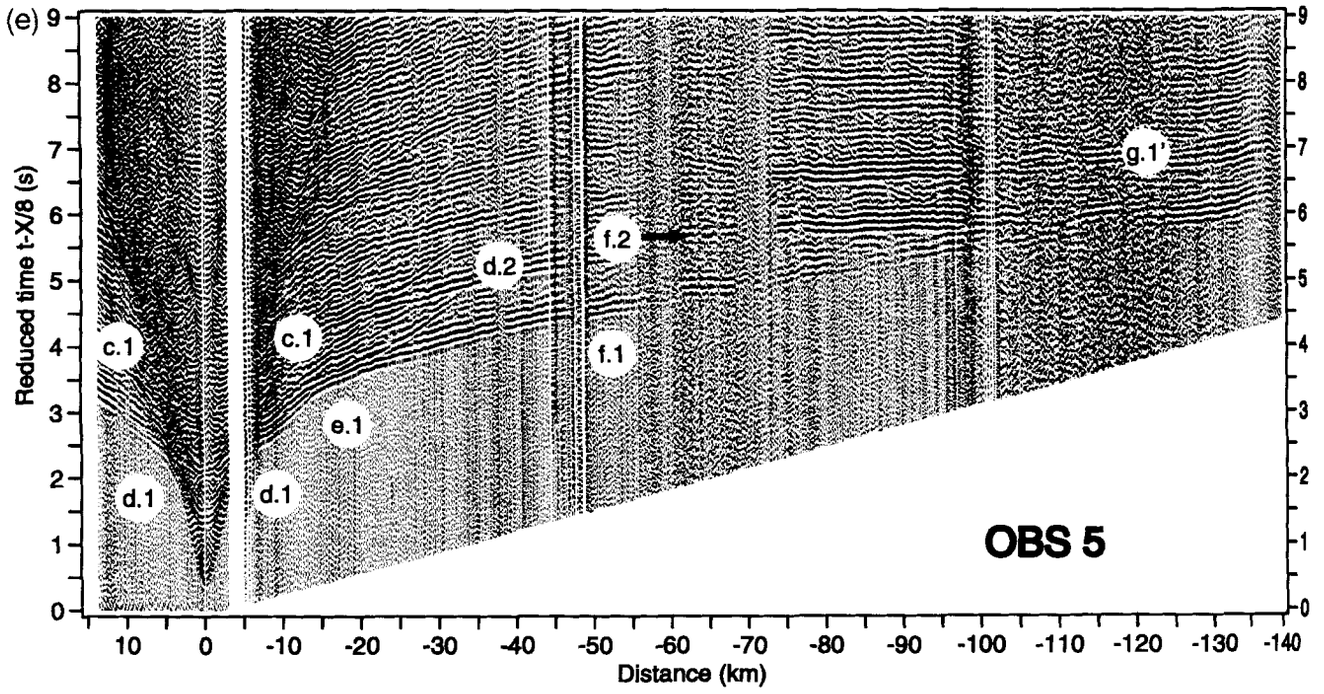

Figure 7. (*Continued.*)

layer C is 1.2 km thick, with velocities ranging from 2.3 to 2.6 km s^{-1}. Layer D is 1.2–2.3 km thick, with velocities ranging from 3.8 to 4.9 km s^{-1}. The latter rather high velocities might be ascribed either to volcanic material interlayered with sediments (Munschy & Schlich 1987; Charvis *et al.* 1993), or to low-density lava flows (e.g. altered and/or highly porous volcanic rocks), as previously postulated by Recq & Charvis (1986) for the shallow structure of the Kerguelen Isles.

Layer E, the upper igneous crust, is 2.1–3.0 km thick, with velocities ranging downwards from 5.0 to 6.1 km s^{-1}. The shape of the traveltime curve and the high amplitude of waves refracted in this layer (Fig. 7) are consistent with the high velocity gradient, 0.3–0.4 s^{-1}, computed from the inversion. The velocities in the upper crust (layer E) are mostly within the range of those encountered in oceanic layer 2 (White *et al.* 1992).

The lack of reflected waves from the layer E–F interface and the smooth transition between both arrivals (e.1) and (f.1) (Fig. 7, Table 1) are consistent with a velocity jump of less than 0.7 km s^{-1} across the layer E–F interface (Fig. 11). This interface is marked by a sharp drop in the velocity gradient from 0.3 s^{-1} down to 0.05 s^{-1}.

Refracted waves travelling the lower crust (f.1) are observed as first arrivals beyond 25 km to a maximum offset of roughly 125 km, emphasizing the great thickness of layer F and its low velocity gradient as well. This layer is devoid of any internal discontinuity and its top is quite horizontal. Since the value of velocity gradient in the lower crust is crucial to calculate accurately the velocity at the crust–mantle boundary and the Moho depth, we analyse the uncertainty in velocity gradient by comparing T_{rms} and χ^2 of a series of velocity models (Fig. 10). An average velocity gradient of 0.054 s^{-1}, with $T_{rms} = 0.065$ and $\chi^2 = 1.42$ s, is computed from the traveltime inversion of (f.1). This calculation was carried out for velocity gradients ranging from 0.01 s^{-1} to 0.09 s^{-1} (Fig. 10). The most reliable gradient is that which minimizes T_{rms} and χ^2 while allowing rays to be traced to the maximum number of traveltime picks. Gradients between 0.054 s^{-1} and 0.067 s^{-1} are suitable, the most accurate value being 0.058 s^{-1} (Fig. 10). We also compared the amplitudes of first arrivals from OB

Table 1. Identification of waves observed on the different seismic sections. The wave code n.1 is assigned to a refraction within the layer labelled N and the wave code n.2 to a reflection from the bottom of layer N (see also Figs 7 and 9).

Wave code	OBS sections	Source–receiver offset (km)	Apparent velocity (km s^{-1})	Description
c.1	all	0–10	~2.5	refracted in C
d.1	all	0–10	~4.5	refracted in D
d.2	all	20–35		reflected from top of E
e.1	all	10–25	~5.5	refracted in E
f.1	all	25–125	~6.8	refracted in F
f.2	3 & 5	variable		reflected from top of G
g.1'	5	100–130	~8.3	multiple of refracted in G
h.	1 & 2	variable		?

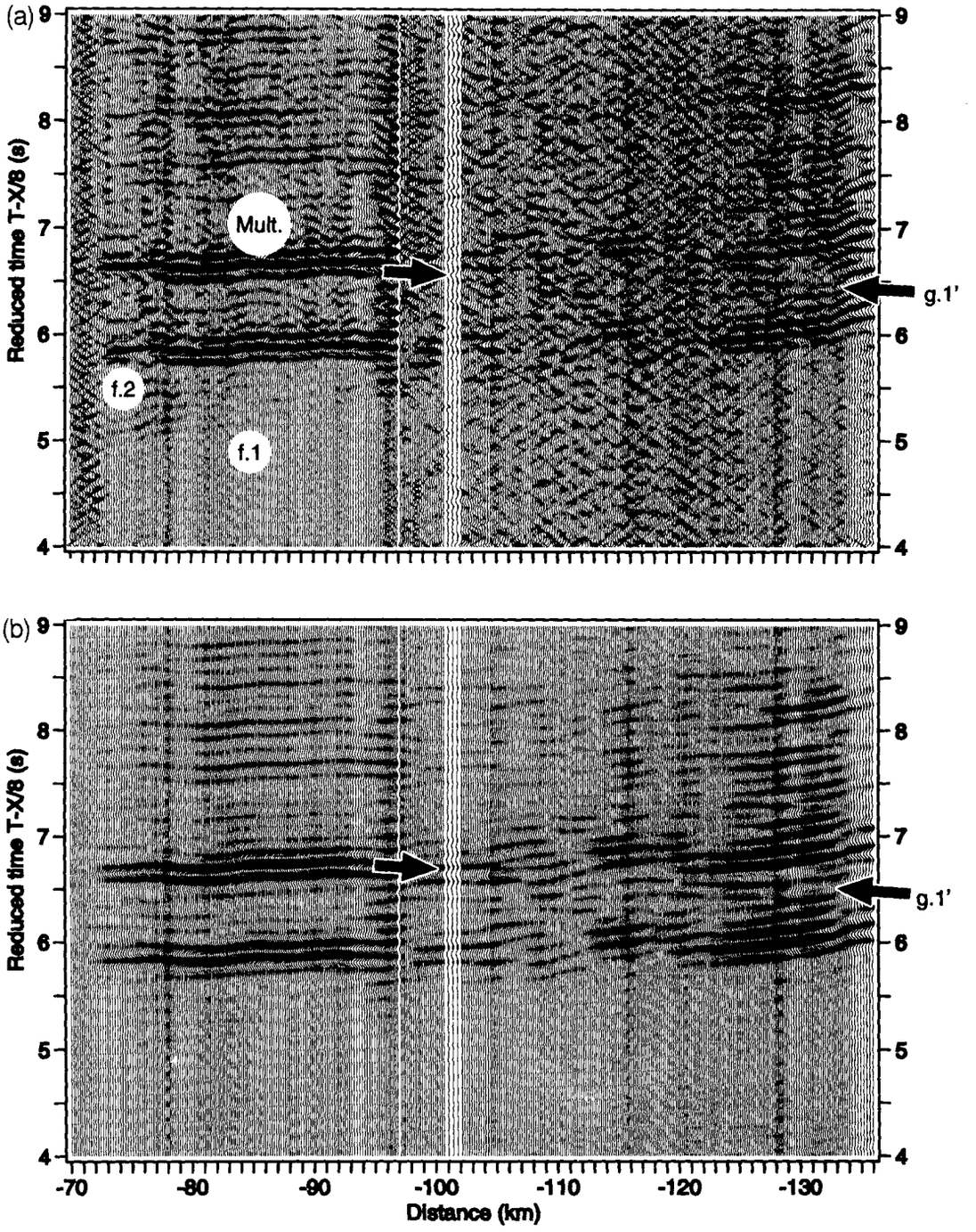

Figure 8. Detail of the recorded section from OBS 5 at distances ranging from 70 to 135 km. The reduction velocity is 8 km s^{-1}. (a) The upper section was f-k filtered. Waves refracted within the lower crust (f.1), *PmP* waves reflected from the Moho (f.2), and the multiple of *PmP* (Mult.) are clearly visible. The multiple bears a very high amplitude and has a traveltime delay of 0.75 s. The multiple is ascribed to a downward reflection of the *PmP* from the top of the water column. The quasi-linear arrival, denoted by closed arrows and labelled (g.1′), has an apparent velocity of roughly 8.3 km s^{-1}. This high apparent velocity and the traveltime relative to the multiple of *PmP* led us to interpret this seismic wave as the multiple of *Pn* (refracted within the upper mantle). The critical point is at a range of 70 km or so; amplitudes reach their greatest values between 73 and 97 km from the receiver. Amplitudes of *Pn* are probably too low to be observed. (b) The lower section was filtered using the interspectral matrix to enhance the coherence of arrivals close to horizontal (Glangeaud & Latombe 1983). The multiple of *Pn* (g.1′), indicated by close arrows, is emphasized whereas f.1 is strongly attenuated.

Table 2. 'Stopping' criteria for the final model are summarized in this table. See Table 1 for wave codes. N: number of data points used; T_{rms}: rms traveltime residual. Parameters used for the inversion; damping factor D = 1; uncertainty estimate on the model velocity value $s_v = 0.1\ km\ s^{-1}$; uncertainty estimate on boundary $s_z = 0.5$ km (see Zelt & Smith 1992).

Wave code	N	T_{rms}	χ^2
c.1	175	0.091	0.841
d.1	298	0.035	0.481
d.2	150	0.288	3.707
e.1	296	0.046	0.857
f.1	1710	0.065	1.434
f.2	265	0.051	0.486
g.1′	86	0.017	0.114
all waves	1970	0.088	1.292

record sections 1 and 5 with those computed from synthetic seismograms for different velocity gradients within layer F (Fig. 12). On OBS record section 1 (Fig. 7a), computed amplitudes comply with those observed on (f.1), assuming a velocity gradient ranging from 0.046 to 0.063 s^{-1} at distances ranging from 30 km to 70 km (Fig. 12). However, at distances from 70 km to 130 km, the attenuation-free amplitude ($Q = 1000$) is slightly too high and a better fit is obtained assuming a rather high attenuation ($Q = 400$) in layer F (Fig. 12). On OBS record section 5, a good fit is also obtained assuming a gradient of 0.054 s^{-1} and $Q = 400$ at distances from 30 to 90 km. At greater distances, the observed amplitudes are larger than the computed ones. Wide-angle *PmP* reflections (f.2) observed on OBS section 5 display high amplitudes at distances ranging from 90 km to

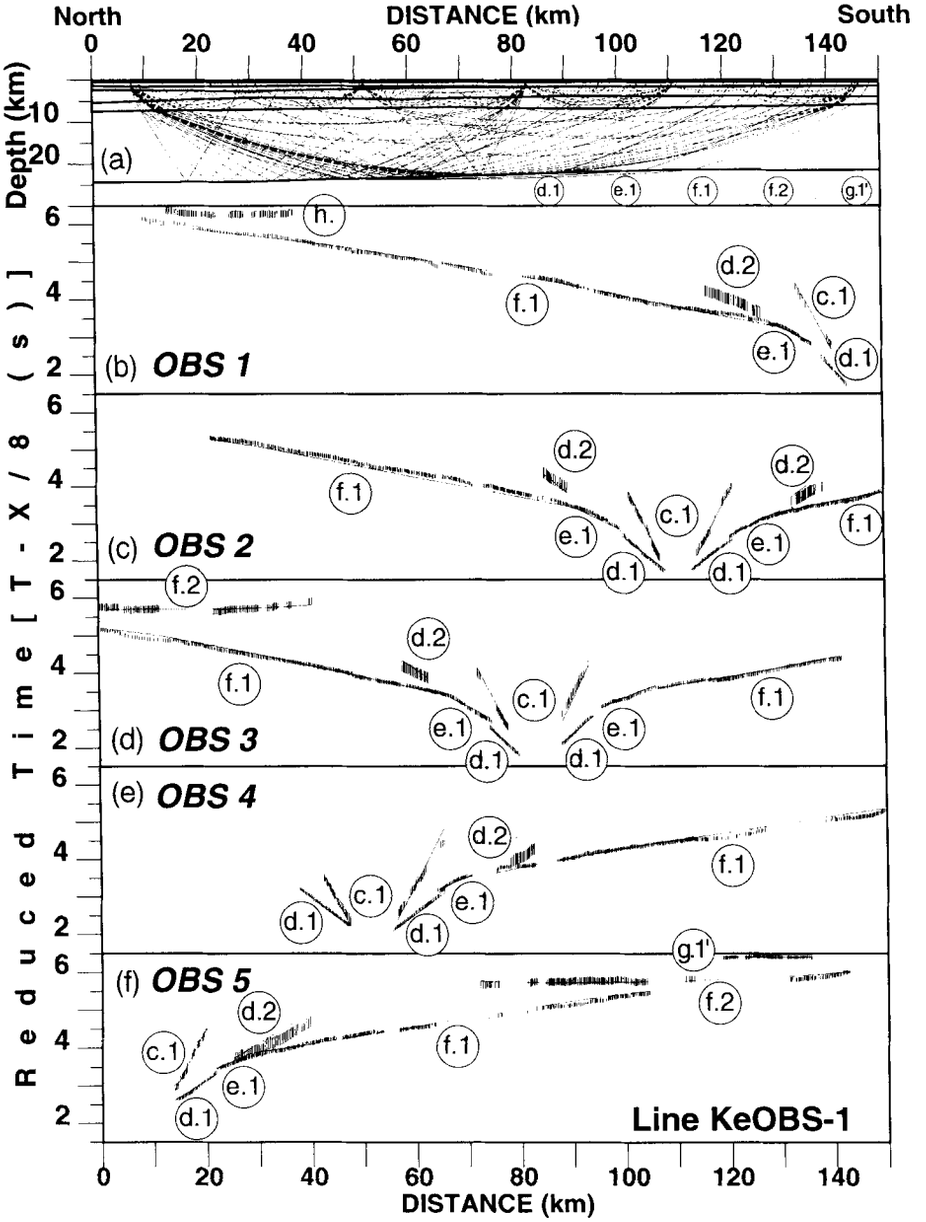

Figure 9. (a) Actual ray path coverage. Each ray group is characterized by different dashed lines labelled d.1. to g.1′ (except c.1, this layer being too thin). (b)–(f) Comparison between digitized traveltimes denoted by vertical bars and computed traveltimes denoted by solid lines for the five OBSs. The bar length is twice the uncertainty used in the inversion, usually 0.05 s for traveltime picks of first arrivals, 0.10 s for traveltime picks of second arrivals. Seismic phases are labelled from (c.1) to (h) as shown in Table 1.

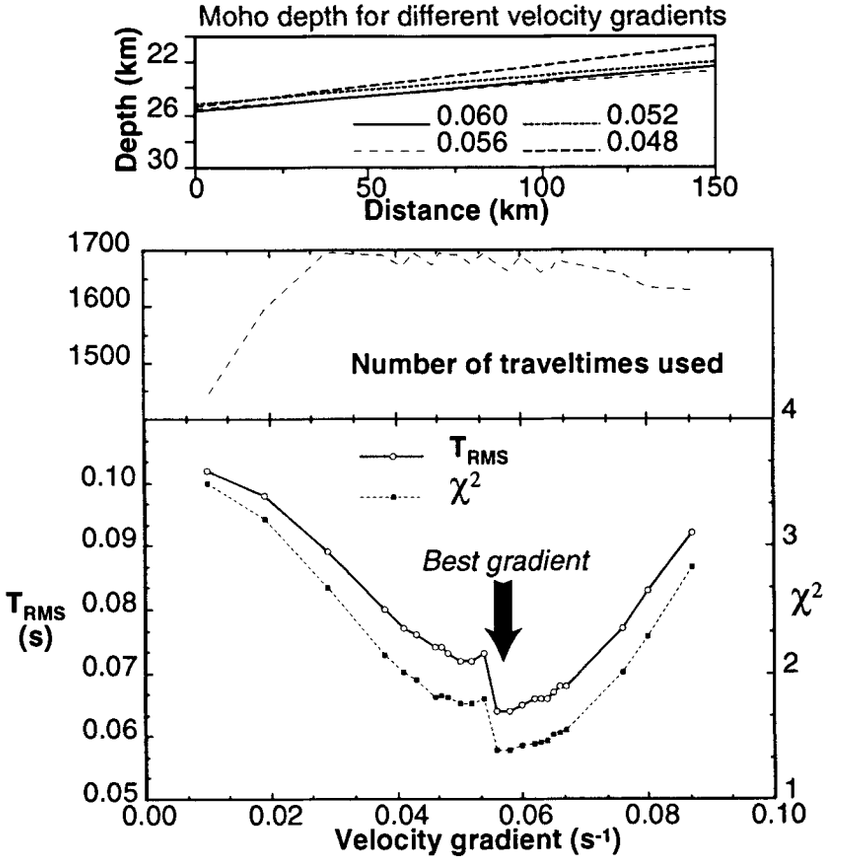

Figure 10. Analysis of the uncertainties in the computed lower crustal velocity gradient and the Moho depth. The T_{rms} misfit and χ^2 are calculated according to values of the velocity gradients within the lower crust (layer F). The best velocity gradient is $0.054\,s^{-1}$ with an uncertainty of approximately $\pm 0.01\,s^{-1}$. The variation of the Moho depth is ± 1 km, as the velocity gradient in the lower crust varies from 0.048 to $0.060\,s^{-1}$.

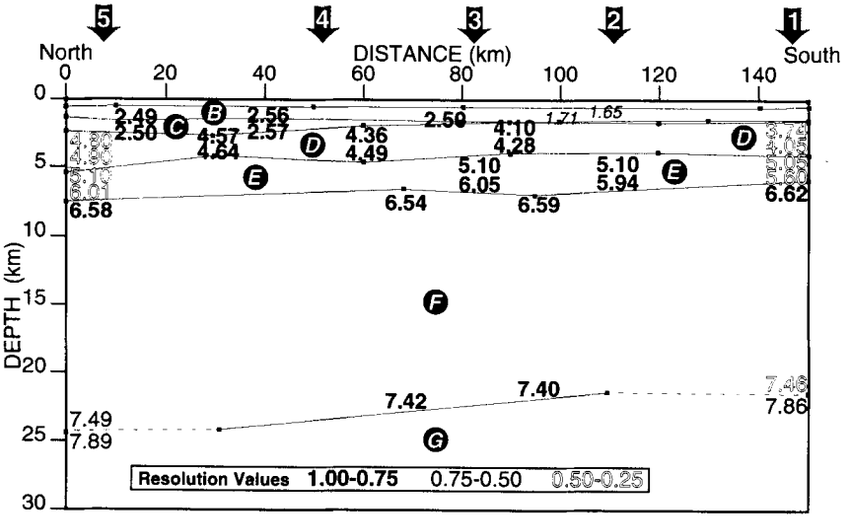

Figure 11. Final model inferred from traveltime inversion from the five sections of KeOBS1 applying the Zelt & Smith method (1992). Each velocity node is labelled according to computed velocities, except for layers A and B whose average velocities are indicated. Black squares denote interface nodes used for the inversion. Resolution values of the velocity nodes according to Zelt & Smith (1992) are shown: bold numbers are ascribed to resolution values falling between 1.00 and 0.75; normal numbers to those between 0.75 and 0.50; and white numbers to those between 0.50 and 0.25.

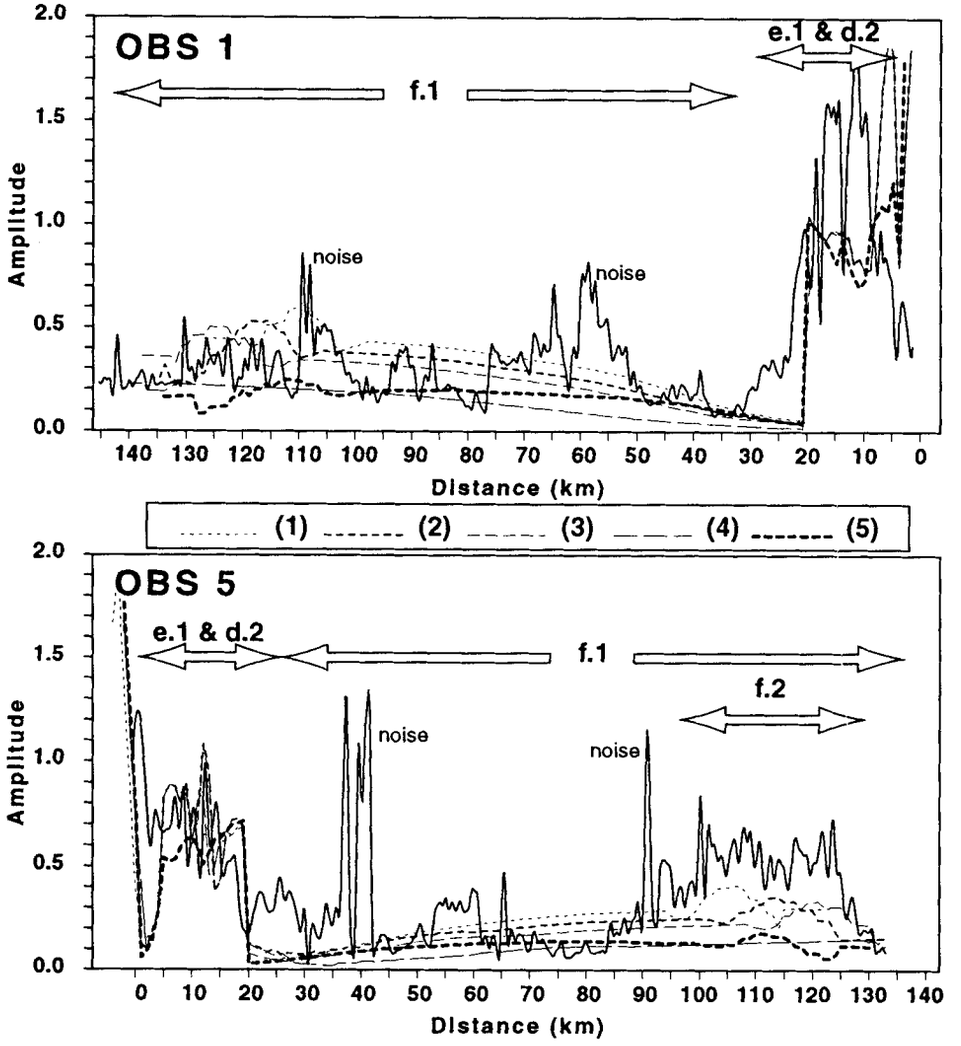

Figure 12. Variations of the maximum amplitude (scaled with distance) of the first wave train along line KeOBS1 for OBSs 1 and 5. The plain curve denotes observed amplitudes. The dashed curves are from synthetic seismograms (using the zero-order asymptotic ray theory) according to various velocity gradients in the lower crust (layer F). (1) 0.029 s^{-1}, $Q = 1000$ (no attenuation); (2) 0.046 s^{-1}, $Q = 1000$; (3) 0.054 s^{-1} $Q = 1000$; (4) 0.054 s^{-1}, $Q = 400$; (5) 0.063 s^{-1}, $Q = 1000$.

130 km (Figs 7e and 12). These amplitudes are not properly modelled by a single sharp discontinuity.

In the final model (Fig. 11), 0.054 s^{-1} has been selected as the minimum acceptable velocity gradient in layer F (Fig. 10). This value is consistent with amplitudes of (f.1) if we assume $Q = 400$ in layer F (Fig. 12). The velocity in the lower igneous crust (layer F) increases from roughly 6.6 km s^{-1} at the top to 7.4 km s^{-1} or so at the crust–mantle boundary. These velocities are within the range of those observed within oceanic layer 3, 6.6–7.6 km s^{-1} (White *et al.* 1992). The critical distances of about 70 km on the OBSs 3 and 5 record sections, computed from ray tracing, comply with the observed maximum amplitude between 70 and 90 km (Figs 7c and e). The Moho depth was calculated from *PmP* waves (f.2) observed on OBS sections 3 and 5 and from the multiple of the *Pn* wave observed on OBS section 5 (Figs 7c, e and 8). Thus, the Moho depth is calculated accurately at distances ranging from 40 to 100 km (Figs 9 and 11). As the gradient in layer F increases from 0.048 s^{-1} to 0.060 s^{-1}, the deepening of the Moho is less than 1 km (Fig. 11). The velocity in the upper mantle is based upon the simultaneous inversion of phases (g.1′) and (f.2), postulating no lateral velocity variation (1-D model) and a constant gradient of 0.1 s^{-1} in layer G. A *Pn* (multiple) is observed on OBS section 5 only (Fig. 7e) and the Moho is constrained by *PmP* waves observed on OBS sections 3 and 5 (Figs 7c and e). A true velocity of 7.9 km s^{-1} in the upper mantle was then calculated. The absence of *Pn* first arrivals along line KeOBS 1 (northern Kerguelen Plateau), when high-energy *Pn* waves have been recorded using the same devices (OBSs and seismic sources) in the Raggatt Basin at the northern end of the southern Kerguelen Plateau (Operto, 1995; Operto & Charvis 1995), substantiates the occurrence of a low velocity gradient within the upper mantle below the Kerguelen–Heard Plateau, as previously noticed for the Kerguelen Isles (Recq *et al.* 1990).

Unexpectedly, the rather uniform thickness (17 km) of the lower crust is far greater than that observed below the Kerguelen Isles (7–9 km). The crustal thickness below KeOBS1 is about 23 km, greater than below the Kerguelen

Isles. Although the Moho depth reaches 19–20 km at the centre of the archipelago, the great variability of crustal thickness below the archipelago makes the average thickness of the crust close to 17–19 km, including the mean elevation of the archipelago, 0.3 km (Rouillon 1963; Charvis 1984). The igneous section of the crust below the Kerguelen–Heard Plateau ranges from 18 to 21.5 km, depending on whether or not the composition of layer D is either mostly volcanic or mostly sedimentary. *PmP* waves observed on OBS sections 3 and 5 (Figs 7c and e) lead us to model the Moho at a depth of 21.5–24.0 km below sea-level. Nevertheless, we postulate the occurrence of major lateral variations of the Moho reflectivity to take into account the lack of *PmP* on OBS sections 1, 2 and 4 (Figs 7a, b and d), the low amplitudes of *PmP* on OBS section 3 (Fig. 7c), and the high energy of *PmP* on OBS section 5 (Fig. 7e). The crust–mantle boundary is modelled as a sharp discrete interface that is probably discontinuous below the Kerguelen–Heard Plateau. However, the existence of a progressive transition zone, as described beneath the Kerguelen Isles, is dubious. The crustal structure below the Kerguelen–Heard Plateau bears some semblance, except for the total crustal thickness, to the deep crustal structure of Josephine Seamount, located at the north-easterly end of the Madeira-Tore Rise in the eastern North Atlantic Ocean. There the velocity with the lower crust increases steadily to 7.4 km s^{-1} down to the abrupt crustal–mantle boundary at a depth of 17 km (Peirce & Barton 1991).

INTERPRETATION

Our results show that the northern Kerguelen Plateau, including the Kerguelen Isles, is oceanic in character, although assumed velocities at the base of the crust below the Kerguelen Plateau are rather high to be satisfactorily assigned to standard oceanic layer 3. Unlike the Kerguelen Isles, where crustal thickening is caused mostly by layer 2, crustal thickening occurring below the Kerguelen–Heard Plateau is caused by an up to 17 km thick layer 3, four times thicker than below oceanic basins. Layer 2 below the Kerguelen–Heard Plateau is on average 5.5 km thick, if layer D is aggregated with layer E as a section of oceanic layer 2, making the basalt only two times thicker than that encountered below deep ocean basins.

Modelling the crust beneath P2-83 (Figs 4a and b) shows that unlike the Rallier du Baty plutonic complex, the Montagnes Vertes plutonic complex outcrops over 1 km^2 but has no lateral extent at depth. Few data are available on seismic velocities within oceanic plutonic complexes. Meanwhile, a recent investigation of the structure of Mont Ross, which caps a plutonic ring complex, indicates velocities ranging from 5.5 km s^{-1} at shallow depth to 6.6 km s^{-1} at a depth of 10 km (Le Roy *et al.* 1993; Recq *et al.* 1994).

In the Kerguelen Isles, at the western end of profile P2-87, velocities of 6.2–6.3 km s^{-1}, higher than those observed in lava flows at shallow depth (Fig. 6a), denote the seaward extension of the Rallier du Baty plutonic complex.

If the seismic velocities within the uppermost lower crust are nearly in the same range below the Kerguelen–Heard Plateau and the Kerguelen Isles, they differ in the lowermost crust, 7.4 km s^{-1} below the submarine plateau, 6.75 km s^{-1} or so below the islands, just over the top of the crust-to-mantle transition zone.

It is well established that hydrothermal processes causing serpentinization can operate at depths of up to several kilometres below the sea-floor (Hess 1955, 1962; Salisbury & Christensen 1978). Velocities which are rather low compared to normal mantle velocities (8.0–8.1 km s^{-1}), either at the base of the crust or within the upper mantle, could be a consequence of water injection in some circumstances (Bowin 1973; Orcutt *et al.* 1975; Lewis & Snydsman 1977; Lewis 1983; Whitmarsh *et al.* 1986). Hence, serpentinized peridotite is suspected. This could cause *P*-wave velocities at the crust–mantle boundary as low as 7.2–7.4 km s^{-1}. Nehlig & Juteau (1988) have shown that at ocean ridges, early hydrothermal circulation may affect the whole crust, down to the petrological mantle. However, several reasons lead us to discard serpentinization of mantle material below the Kerguelen Isles as well as the Kerguelen–Heard Plateau. Hydrothermal circulation to depths of 20 km is doubtful. Serpentinite becomes unstable at temperatures over 540 °C. Bassias *et al.* (1987) have shown from dredges and drilling on the Kerguelen Plateau that well-preserved foraminifera within a recrystallized micrite matrix indicate a rapid recrystallization subsequent to the emplacement of the Plateau, and as the basaltic body was cooling this would have hindered the downward circulation of fluids. Therefore, serpentinization is an unsuitable process to cause low velocities at depths of tens of kilometres below the Kerguelen Plateau and the Kerguelen archipelago as well.

The crust–mantle boundary below the Kerguelen Isles has been modelled by a high-velocity-gradient transition zone bounded by first-order discontinuities, and has been interpreted as 2–3 km thick underplated material (Recq *et al.* 1990). The presence of underplated mantle material added to the crust below the Kerguelen Isles was corroborated by Grégoire *et al.* (1992). They showed from ultrabasic xenoliths collected on the islands that a large amount of melt was trapped below layer 3 preceding alkaline magmatism. Grégoire *et al.* (1994) assigned xenoliths to underplated basaltic magmas.

Velocities of 6.70–6.90 km s^{-1} at the top of layer 3 under the Kerguelen Isles and the Kerguelen Plateau might also be regarded as too low to be assigned to material produced by a mantle plume. However, the downward velocity increase to 7.4–7.6 km s^{-1} within the crust-to-mantle transition zone is quite compatible with that generated by such a process (Fowler *et al.* 1989; White & McKenzie 1989). These latter velocities have been rarely observed below deep-sea oceanic basins (Christensen & Salisbury 1975; White *et al.* 1992). The melt generated by adiabatic decompression may have velocities of 7.2–7.6 km s^{-1} if large quantities of hot picritic melt containing an average of 16 per cent of MgO are produced (McKenzie & Bickle 1988; White & McKenzie 1989). These velocities denote contamination of the lower crust or underplating by such a melt which makes the lower crust up to 17 km thick in the vicinity of a hotspot (Storey *et al.* 1988, 1989; Saunders *et al.* 1990). An elevation of the mantle temperature by 100–150 °C caused by upwelling of the Kerguelen plume may generate such a volume of melt (McKenzie & Bickle 1988).

Sinha, Louden & Parsons (1981), White *et al.* (1987), McKenzie & Bickle (1988), and White & McKenzie (1989) ascribed velocities of 7.2–7.5 km s^{-1} to lower crustal material within provinces bearing peculiar affinities with underplating, as well as to lower crust contaminated by upwelling mantle material. The melting process must be able to generate sufficient melt under normal oceanic ridge spreading centres to produce an 8.3 ± 1.5 km thick igneous crust (White *et al.* 1992), increasing to nearly 25 km where the ridge crosses a hot rising plume (McKenzie & Bickle 1988). These thicknesses are produced by adiabtic upwelling of the mantle with potential temperatures of 1280 °C and 1480 °C, respectively. Conversely, features away from the influence of any hotspot at the time of rifting, such as the Biscay and Galicia margins, are largely devoid of basalt (Whitmarsh *et al.* 1986; Boillot *et al.* 1987; Recq, Whitmarsh & Sibuet 1991; White 1992; Whitmarsh *et al.* 1993).

Using the potential temperature–crustal thickness relationships of McKenzie & Bickle (1988), redrawn by ourselves (Fig. 13), the potential temperature related to 18 km thick igneous material (after removing Plio-quaternary sediments) is 1400 °C, a rather low value, compared with 1480 °C to produce velocities of around 7.2 km s^{-1} and a thickness of 25 km of igneous material (McKenzie & Bickle 1988). This is probably the main reason for the thin underplated layer below the Kerguelen Isles and the low melt output rate (35 m^3 s^{-1}; Saunders *et al.* 1990).

According to McKenzie & Bickle's hypothesis (1988), the potential temperature below the Kerguelen–Heard Plateau would be 1440–1450 °C for 21.5 km of melt, a little bit lower than 1480 °C to produce 25 km of melt and velocities of 7.2–7.4 km s^{-1} (McKenzie & Bickle 1988).

Higher velocities than usual for a melt thickness of 21.5 km at the base of the crust below the Kerguelen–Heard Plateau would be a consequence of a higher potential temperature than normal (and a higher output rate as well) producing extra melt to thicken layer 3 below the Kerguelen–Heard Plateau between Kerguelen and Heard Islands.

The profile KeOBS1 was shot in the vicinity of the north-eastern flank of the Kerguelen Plateau (Fig. 2), not far from the site where Wicquart & Fröhlich (1986) showed from cores and dredges that collected samples, mostly Cretaceous in age, are unlike the Kerguelen Isles in being free of recent volcanism. The base of the series is roughly 100–120 Ma old (Albian–Hauterivian). Storey *et al.* (1992) and Whitechurch *et al.* (1992) stated on the basis of radiometric dates that the formation of the Kerguelen Plateau was completed 110 Ma ago. At the Kerguelen Isles, volcanism was still active a few thousand years ago. Some fumaroles have been discovered on the western region of the main island. The long-lasting melt generation may produce a higher volume of melt. The lack of recent magmatism beneath the Kerguelen Plateau leads us to regard the crustal structure highlighted by profile KeOBS1 as a reliable indication of the primitive domain of the

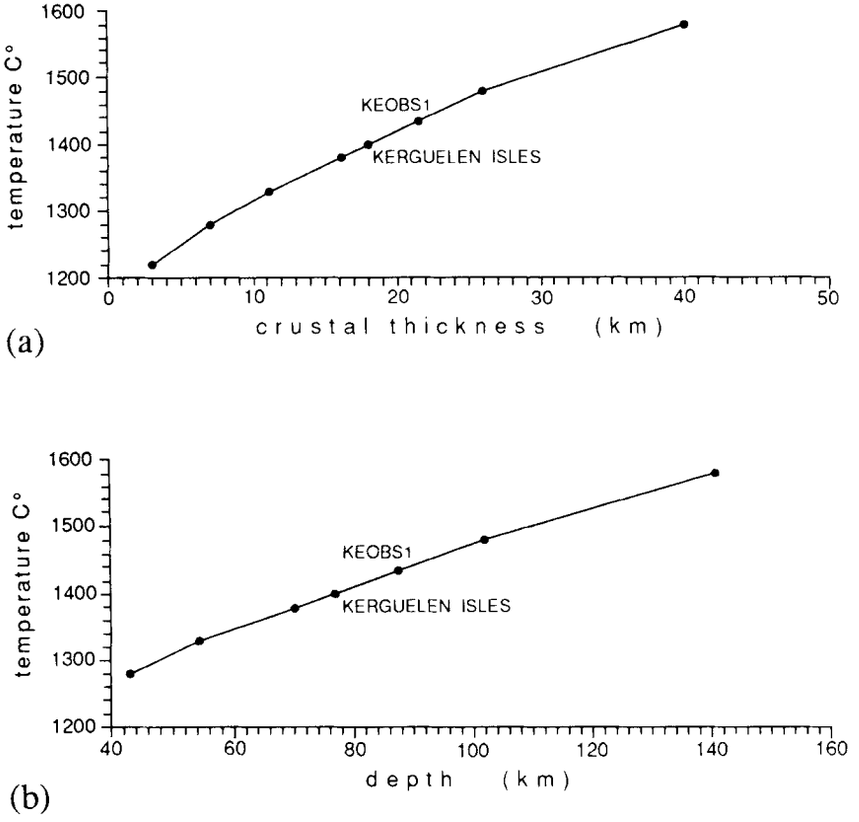

Figure 13. (a) Potential temperature versus produced melt thickness (layer 2 + layer 3) function subsequent to mantle adiabatic decompression. (b) Potential temperature plotted as a function of the maximum depth of partial melting. These figures, have been redrawn from data presented by McKenzie & Bickle (1988). Data related to the Kerguelen Isles and the Kerguelen–Heard Plateau (KEOBS1) are plotted according to igneous material thicknesses of 18 km and 21.5 km respectively.

Kerguelen–Heard Plateau contemporaneous with continental break-up. The Rajmahal Plateau and the Kerguelen Plateau were contiguous 110 Ma ago above the Kerguelen–Heard mantle plume (Kent 1991), but, according to Müller and Royer & Lawver (1993), the Rajmahal Traps may not have been directly produced by the Kerguelen hotspot. However, if the mantle plume affected a 2000 km diameter area of rifted continental and oceanic crust, both the Rajmahal Traps and the Bunbury basalts (western Australia) may have been generated as a result of enhanced decompression melting according to White & McKenzie's model (1989).

The potential temperature–depth graph (Fig. 13b) shows that, above plumes, melting occurs in the upper mantle down to a depth of 78 km below the Kerguelen Isles, in rather good agreement with depths of 76 km and 81 km for the compensation level, calculated by Recq & Charvis (1987) and by Marks & Sandwell (1991), respectively. The latter value is ascribed to the density of mantle material depleted by extraction of a huge quantity of basalt. The thickness of layer 2 below the islands is up to 9 km, compared with 3–5 km beneath the Kerguelen–Heard Plateau. Below the Kerguelen–Heard Plateau, melting would occur down to a depth of 88 km.

Earlier studies (see references in Table 3) showed that the velocity below aseismic ridges falls in the range of 8.0–8.3 km s^{-1}. Recent modelling of the crustal structure of submarine plateaux based on synthetic seismograms is very scarce (listed in White *et al.* 1992, two or three entries only). Most available data were published in very early papers, in which *Pn* velocities and Moho depths are computed from traveltime analysis only. In Table 3, a closer examination of some data extracted from Coffin, Rabinowitz & Houtz (1986) shows that velocities ascribed to the mantle range from 7.5 to 8.1 km s^{-1}. Data from the Ontong Java Plateau (Hussong *et al.* 1979) were not reported in Table 3, the Moho depth being questionable. A 20 km thick 'transition zone' with a velocity of 7.6 km s^{-1} is found below layer 3. The occurrence of such a low velocity below layer 3 is usual within submarine plateaux.

Table 3. h_o: water depth (km), h_c: crustal thickness (km).

	h_o	h_c	
SEYCHELLES	0.05	31.95	Matthews & Davies (1966)
A	1.50	23.76	Hales & Nation (1973)
B	2.20	22.80	Goslin, Recq & Schlich (1981)
RAGGATT	1.75	22.15	Operto & Charvis (1995)
C	1.97	21.58	Francis & Raitt (1967)
D	2.00	20.56	Goslin, Recq & Schlich (1981)
E	1.90	20.50	Sinha, Louden & Parsons (1981)
F	2.40	19.76	Hales & Nation (1973)
G	2.90	18.60	Coffin, Rabinowitz & Houtz (1986)
H	1.97	18.30	Hales & Nation (1973)
I	2.50	18.01	Hales & Nation (1973)
J	2.63	16.49	Coffin, Rabinowitz & Houtz (1986)
K	2.06	16.60	Francis & Shor (1966)
delcano	1.90	15.60	Goslin, Recq & Schlich (1981)
L	1.98	15.32	Francis & Shor (1966)
M	2.50	15.06	Curray et al. (1977)
N	3.23	14.21	Curray et al. (1977)
O	3.15	13.81	Francis & Shor (1966)
Q	3.42	11.84	Coffin, Rabinowitz & Houtz (1986)
R	3.56	11.28	Coffin, Rabinowitz & Houtz (1986)
S	3.50	11.00	Hales & Nation (1973)
T	3.83	10.36	Coffin, Rabinowitz & Houtz (1986)
U	3.69	9.98	Coffin, Rabinowitz & Houtz (1986)
V	3.60	9.90	Francis, Davies & Hill (1966)
W	3.40	9.74	Curray et al. (1977)
X	3.84	9.55	Ludwig et al. (1968)
Y	3.81	9.46	Hales & Nation (1973)
Z	4.00	9.04	Coffin, Rabinowitz & Houtz (1986)
KEOBS1	0.55	23.48	This article
KERG1	0.00	19.00	Recq et al. (1991)
KERG2	0.00	17.00	Recq & Charvis (1986)
S2	1.30	13.44	Goslin, Recq & Schlich (1981)

$h_o = -0.1545\, h_c + 5.147$

For Airy compensated structures, the water depth is a linear function of the crustal thickness:

$$\delta h_c = -\delta h_o(\rho_m - \rho_o)/(\rho_m - \rho_c)$$

where, δh_c and δh_o are differences in crustal thickness and in water depth, respectively, between two Airy compensated structures, ρ_m is the density of the upper mantle, ρ_o is the density of the seawater, and ρ_c is the mean density of the crust.

We have plotted (Fig. 14) the water depth–crustal thickness function for various submarine thickened crusts (>8 km) at various places in the Indian Ocean (Table 3).
(>8 km) at various places in the Indian Ocean (Table 3).

Notwithstanding some peculiar exceptions, such as the southern domain of the Madagascar Plateau, this relationship is quite linear and denotes an Airy-type compensation for most of these features. The southern Madagascar Plateau (Table 3, S2) could experience subsidence which has been active since the Lower Miocene (Schlich *et al.* 1974; Denis-Clocchiatti & Leclaire 1978). The linear relationship between water depth and crustal thickness for some oceanic plateaux of the Indian Ocean has already been established (Recq & Goslin 1981), but data on the deep structure of the Kerguelen–Heard Plateau, the Kerguelen Isles and the Raggatt Basin were not available at that time. Unlike the Raggatt Basin (RAGGATT) in the southern Kerguelen Plateau (Operto & Charvis 1995; Operto 1995), data related to the Kerguelen Isles (KERG1 & 2) and the Kerguelen–Heard Plateau (KEOBS1) do not fit the general trend (Fig. 11, Table 3), so that we reject an Airy-type compensation for both features. This latter statement is substantiated by geoid studies. Fig. 11 shows that crustal thickening below the Kerguelen–Heard Plateau and the Kerguelen Isles is insufficient to achieve local Airy-type isostatic compensation, though the crust beneath submarine plateaux is far thicker than below ocean basins. However, gravity measurements (Fig. 3) carried out throughout the Kerguelen Isles (Rouillon 1963; Charvis 1984; Recq & Charvis 1986), and over the southern Kerguelen Plateau (Houtz *et al.* 1977; Li 1988), showed that both features are nearly compensated. Moreover, the involvement of low-density mantle material to achieve the compensation of the Kerguelen Isles and the northern Kerguelen–Heard Plateau appears to be a quite reasonable hypothesis, in good agreement with a low, and even possibly negative, velocity gradient within the uppermost mantle. Marks & Sandwell (1991) investigated the relationships between geoid height and topography for several oceanic plateaux and swells to determine the mode of compensation. Assuming a two-layer Airy model, these authors computed a Moho depth of 19.5 km, and a mantle root extending to a depth of 81 km for the northern Kerguelen Plateau. Low velocities, and even a negative velocity gradient within the uppermost mantle down to 100 km depth below Broken Ridge, play a key role in

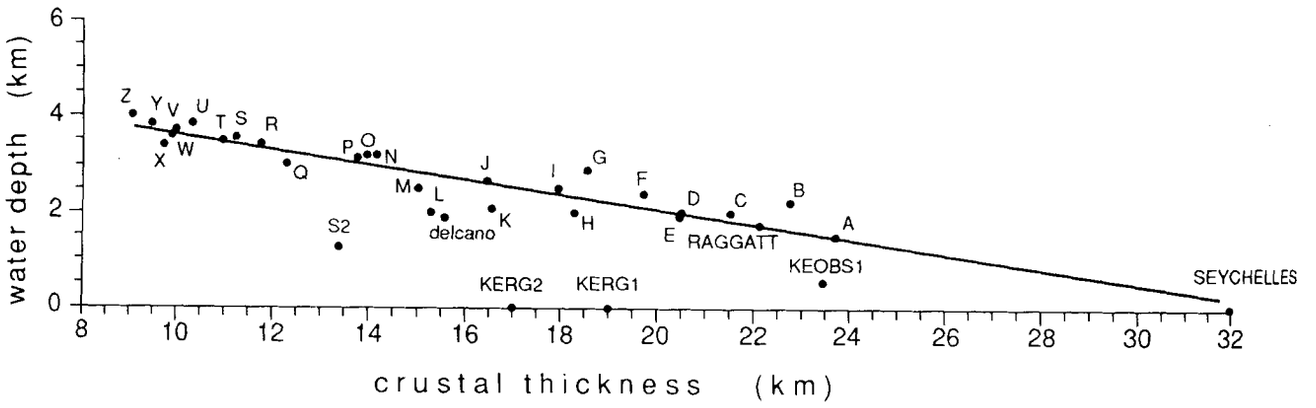

Figure 14. Water depth–crustal thickness relationship plotted from refraction data extracted from the literature on thickened crust (>8 km) at various places in the Indian Ocean. Data are labelled as shown Table 3. Unlike the Kerguelen–Heard Plateau and the Kerguelen Isles, the compensation of the Raggatt Basin (southern Kerguelen Plateau) is achieved according to an Airy-type model. KEOBS1: Kerguelen–Heard Plateau; KERG: Kerguelen Isles; S2: Southern Madagascar Plateau. The regression line has been calculated excluding data which largely differ from the general trend (S2, KERG1 and 2, KEOBS1). However, delcano (Delcano Rise, western Crozet Plateau), which slightly differs from the regression line, has been taken into account.

providing the isostatic conditions of the Ninetyeast Ridge (Souriau 1981).

CONCLUSION

Refraction data collected through the Kerguelen Isles, and over the Kerguelen–Heard Plateau, exhibit an oceanic-type velocity–depth structure for both areas. The main purpose of the experiments carried out in 1983 and 1987 across the Kerguelen archipelago was to acquire some information on the deep structure of the Kerguelen Isles and consequently on the overall structure of the Kerguelen–Heard Plateau. The KeOBS experiment proved that the assumption that the crustal structures are similar below the Kerguelen–Heard Plateau and the Kerguelen Isles is incorrect. The profile KeOBS1 emphasizes basic differences between the crustal structure below the Kerguelen Isles and the Kerguelen–Heard Plateau, and suggests that both features have distinct origins. Geochemical studies (Giret 1983; Gautier *et al.* 1990) outlined an intraplate origin for newly generated basalts of the Kerguelen Isles. The existence of underplated mantle material at the base of the lower crust appears to be doubtful below the Kerguelen–Heard Plateau. Velocities of 7.2–7.4 km s^{-1} and the difference in thicknesses of layer 3, which exceeds 10 km below the Kerguelen–Heard Plateau and the Kerguelen Isles, may be a consequence of contamination of the lower crust by mantle material. Unlike the Kerguelen–Heard Plateau, the increase in crustal thickness below the Kerguelen Isles (and the northernmost domain of the Plateau ?) lies chiefly within layer 2.

The velocity–depth behaviour below the Kerguelen Isles is similar to that found below intraplate oceanic islands such as Hawaii where the basaltic layer is up to 8 km thick (Ryall & Bennett 1968; Zucca, Hill & Kovach 1982; Watts *et al.* 1985). Below the Kerguelen and Hawaiian Islands, a transition zone occurs at the crust–mantle boundary. Ten Brink & Brocher (1987) and Watts & ten Brink (1989) attribute the deep Moho discontinuity (18 km) beneath Oahu to up to 4 km of material added to the base of the flexed crust during the late stage of volcanic loading.

The low velocity gradient, or even a possible negative gradient, within the upper mantle below the Kerguelen Isles substantiates the presence of low-density mantle down to a depth of 76–78 km. This low-density material allows the achievement of local isostatic compensation, already advocated by Charvis (1984), Recq & Charvis (1987), and Marks & Sandwell (1991). These latter authors, from geoid data, proposed a crustal thickness of 19.5 km and the occurrence of low-density material down to 81 km deep. Notwithstanding some discrepancies between data related to the crust–mantle boundary below the Kerguelen Isles, the depth of the Moho appears unexpectedly to be smaller below the archipelago (15–20 km, varying greatly with locality, and below the northern domain as well ?) than below the Kerguelen–Heard Plateau (23.5 km). Houtz, Hayes & Markl (1977) postulated that the Moho would be 23 km deep in order to achieve the isostatic compensation of the southern Kerguelen Plateau. The crustal structure below the profile KeOBS1 provides a good indication of the upper lithosphere of the former Cretaceous Kerguelen Plateau (Wicquart & Fröhlich 1986).

It is reasonable to state that the structures of the Kerguelen Isles and the Kerguelen–Heard Plateau highlight distinct processes of emplacement for these features. These processes are compatible with the genesis of the Kerguelen–Heard Plateau during Cretaceous time, and with the northernmost region of the plateau and the Kerguelen Isles in the last 45 Ma. According to Saunders *et al.* (1990), the volcanic output rate of the Kerguelen Plateau and the Ninetyeast Ridge was time-dependent and decreases to a very low value. This hypothesis suggests a close kinship between structures and output rates (as well as the potential temperature at the initiation of melt generation). Furthermore, the northernmost termination of the Kerguelen Plateau, and the archipelago, were emplaced in the vicinity of a slow-spreading 22 mm yr^{-1} ridge (Royer & Coffin 1992), and then moved into an intraplate situation.

A recent seismic tomography profile shot in south-western Iceland across the Mid-Atlantic Ridge active spreading centre exhibits a 24 km thick crust (Bjarnason *et al.* 1993).

According to these authors, the crust is split into three layers: the upper crust, midcrust and lower crust. Within the 0.7–2.5 km thick upper crust velocities range from 2.5 to 5.0 km s^{-1}. Within the 2.0–4.5 km thick midcrust velocities range from 5.0 to 6.6 km s^{-1}. The lower crust has an average thickness of 17.5 km and its top is defined by a sharp drop in the velocity gradient where the velocity reaches 6.5 km s^{-1}. Velocities range downwards from 6.5 to 7.2 km s^{-1}. Velocities and thicknesses of this three-layer crust are similar to those determined for layers C, D and E, respectively, at the KeOBS1 profile.

The crust below Iceland has an age of 0 Ma, and below the Kerguelen Plateau it is 100–120 Ma. However, these two features are strikingly similar. The high temperature suspected within the Icelandic crust may have been overestimated or have had little effect upon crustal seismic velocity (Bjarnason *et al.* 1993). Notwithstanding age and thermal regime differences, this comparison strongly supports a similar origin for both structures, the Kerguelen–Heard Plateau being a fossil equivalent of present-day Iceland.

From a compilation of previously published data, Mutter & Mutter (1993) stated that the thickness of layer 2 relative to the whole crustal thickness decreases as the whole thickness increases. Nevertheless, for a similar total thickness, the fraction of crust bearing layer 2 velocities is much greater for crust originating in midplate settings than for crust formed at a spreading centre (Mutter & Mutter 1993). The comparison between the Kerguelen–Heard Plateau and the Kerguelen Isles agrees with this observation. Crustal thickening beneath the Kerguelen–Heard Plateau, which may result from an Iceland-type setting (active spreading centre over a hotspot), is mostly achieved by thickening of layer 3; layer 2 accounts for only 25 per cent of the thickness of the igneous crust. On the other hand, 70 per cent of the igneous crust beneath the Kerguelen Isles exhibits layer 2 velocities, proving that these islands bear most of the characteristics of midplate volcanic islands, despite the initial volcanism near the active Southeast Indian Ridge, and are not definitely representative of the whole Kerguelen Plateau structure.

In summary, refraction lines carried out across the Kerguelen Isles in the 1980s provide consistent models which highlight strong lateral variations in the structure of the crust. Relative thicknesses of oceanic layers 2 and 3, as well as seismic velocities beneath the archipelago, are consistent with an off-ridge emplacement of the Kerguelen Isles (and the northernmost domain of the Plateau) as it moved away from the Southeast Indian Ridge. The seismic refraction profile KeOBS1 (this article), shot between Kerguelen and Heard Islands on the assumed Cretaceous Kerguelen Plateau, emphasizes the basic differences in the deep structure of the archipelago. The 23 km thick crust exhibits a lower crust over 15 km thick, with velocities increasing downwards from 6.5 to 7.4 km s^{-1}. This thickness strongly suggests that the formation of the Kerguelen–Heard Plateau is related to excessive volcanism generated in the vicinity of an active spreading centre. Velocities in the mantle beneath the archipelago, and beneath the Cretaceous Kerguelen–Heard Plateau as well, appear to be as low as 7.70–7.95 km s^{-1}, suggesting that the mantle is involved in the achievement of local isostatic compensation as suggested by geoid studies.

ACKNOWLEDGMENTS

This work would not have reached completion without the considerable financial and technical support of TAAF (Terres Australes et Antarctiques Françaises and the Mission de Recherche) in the field in the Kerguelen Isles, and at sea (MD66/KeOBS cruise). We would especially like to thank Yann Hello (ORSTOM) for his invaluable skilfulness in successfully operating the OBSs at sea without any loss. We also thank the Master Yvon Fercoq (CGM) and crew of M/V *Marion Dufresne* for hard work at sea, Bernard Ollivier (TAAF), the IFREMER-GENAVIR party (Jean Le Pavec, Philippe Le Doze and Jean-Luc Le Philippe) for running seismic sources flawlessly, sea-going colleagues and Jean-Luc Travers (UBO Brest) for redrawing some figures. This research was supported by ORSTOM and CNRS-INSU (DBT5, 'Dynamique globale et croûte océanique épaisse' and 'Tomographie' grants). One of us (MR) is grateful to Dan McKenzie and Robert White (University of Cambridge) for helpful discussions at Bullard Laboratories. We are also grateful to George Spence (University of Victoria) and Martin Sinha (Bullard Laboratories) for their constructive reviews of the original manuscript.

Contributions: INSU No. 652, GEMCO No. 620, IPGP No. 1279.

REFERENCES

Aubert de la Rüe, E., 1932. Etude géologique et géographique de l'Archipel des îles Kerguelen, *Rev. Géogr. Phys. et Géol. Dyn.*, **5**(1).

Bassias, Y., Davies, H., Leclaire, L. & Weis, D., 1987. Basaltic basement and secondary rocks from the southern sector of the Kerguelen–Heard Plateau: new data and their Meso-Cenozoic palaeogeographic implications, *Bull. Mus. natl. Hist. nat., Paris*, **4**, 367–403.

Bjarnason, J.T., Menke, W., Flovenz, O.G. & Caress, D., 1993. Tomographic image of the Mid-Atlantic plate boundary in Southwestern Iceland, *J. geophys. Res.*, **98**, 6607–6622.

Boillot, G., Recq, M., Winterer, E.L. & Leg 120 scientific party, 1987. Tectonic denudation of the upper mantle along passive margins: a model based on drilling results (ODP Leg 103, western Galicia margin, Spain), *Tectonophysics*, **132**, 335–342.

Bowin, C., 1973. Origin of the Ninety East Ridge from studies near the equator, *J. geophys. Res.*, **78**, 6029–6043.

Carter, D.J.T., 1980. *Echo-Sounding Corrections Tables*, formerly Matthew's Tables, 3rd edn., Hydrographic Dept, Admiralty, London.

Charvis, P., 1984. Etude de la structure profonde de deux rides asismiques de l'océan Indien: les plateaux sous-marins de Kerguelen–Heard et de Crozet, *Thesis*, Université Pierre & Marie Curie, Paris.

Charvis, P., Operto, S. & Recq, M., 1992. Lateral inhomogeneities within the Kerguelen Plateau, E.G.S. meeting, Edinburgh, *Ann. Geophys.*, **Suppl. to 10**, C74.

Charvis, P., Operto, S. Recq, M., Hello, Y., Houdry, F., Lebellegard, P., Louat, R. & Sage, F., 1993. Structure profonde du domaine Nord du plateau de Kerguelen (océan Indien austral): résultats préliminaires de la campagne MD66/KeOBS, *C. R. Acad. Sci., Paris*, **316**, 341–347.

Christensen, N.I. & Salisbury, M.H., 1975. Structure and composition of the lower oceanic crust, *Rev. Geophys. Space Phys.*, **13**, 57–86.

Chun, C., 1903. *Aus dem Tiefen des Weltmeeres*, Schilderungen von

der Deutschen Tiefsee-Expedition, Verlag von Gustav Fischer in Jena.

Coffin, M.F., Rabinowitz, P.D. & Houtz, R.E., 1986. Crustal structure in the Western Somali Basin, *Geophys. J. R. astr. Soc.*, **86,** 331–369.

Curray, J.R., Shor, G.G., Raitt, R.W. & Henry, M., 1977. Seismic refraction and reflection studies of crustal structure of the Eastern Sunda and Western Banda Arcs, *J. geophys. Res.*, **82,** 2479–2489.

Denis-Clocchiatti, M. & Leclaire, L., 1978. Mouvements verticaux d'une ride aséismique: une approche sédimentologique, *C. R. Somm. Soc. géol. Fr.*, **5,** 258–261.

Dosso, L. & Murthy, V.R., 1980. A Nd isotopic study of the Kerguelen Island: influence on enriched oceanic mantle sources, *Earth planet. Sci. Lett.*, **48,** 268–276.

Drygalski, E. von, 1912. *Deutsche Süd-Polar Expedition,* Geologie und Geographie, Vol. 2, Georg Reimer, Berlin.

Dziewonski, A.M. & Anderson, D.L., 1981. Preliminary reference Earth model, *Phys. Earth planet. Inter.*, **25,** 297–356.

Edwards, A.B., 1938. Tertiary lavas from the Kerguelen Archipelago, *B.A.N.Z.A.R.E Reports,* A, **2**(5), 72–100.

Fowler, S.R., White, R.S., Spence, G.D. & Westbrook, G.K., 1989. The Hatton Bank continental margin—II. Deep structure from two-ship expanding spread profiles, *Geophys. J.R. astr. Soc.*, **96,** 295–309.

Francis, T.J.G. & Raitt, R.W., 1967. Seismic refraction measurements in the Southern Indian Ocean, *J. geophys. Res.*, **72,** 3015–3041.

Francis, T.J.G. & Shor, G.G., 1966. Seismic refraction in the Northwest Indian Ocean, *J. geophys. Res.*, **71,** 427–449.

Francis, T.J.G., Davies, D. & Hill, M.N., 1966. Crustal structure between Kenya and the Seychelles, *Phil. Trans. Royal Soc., Lond.*, A, **259,** 240–261.

Gautier, I., Weis, D., Mennessier, J.P., Vidal, P., Giret, A. & Loubet, M., 1990. Petrology and geochemistry of the Kerguelen Archipelago basalts (South Indian Ocean): evolution of the mantle sources from ridge to intraplate position, *Earth planet. Sci. Lett.*, **100,** 59–76.

Giret, A., 1980. Carte géologique au 1/50 000 de la péninsule Rallier du Baty, *Com. natl. Fr. Res. Antarct.*, **45.**

Giret, A., 1983. Le plutonisme océanique intraplaque. Exemple de l'archipel de Kerguelen (Terres Australes et Antarctiques Françaises), *Com. natl. Fr. Res. Antarct.*, **54.**

Giret, A. & Lameyre, J., 1983. A study of Kerguelen plutonism: petrology, geochronology and geological implications, in *Antarctic Earth Sciences,* pp. 191–194, Proc. IVth Intern. Symp. on Antarct. Earth Sci., SCAR/IUGS, Adelaide, South-Australia, eds Oliver, R.L., James, P.R. & Jago, J.B., Austr. Acad. Sci. Publ.

Glangeaud, F. & Latombe, C., 1983. Identification of electromagnetic sources, *Ann. Geophys.*, **1,** 245–252.

Goslin, J., 1981. Etude géophysique des reliefs asismiques de l'océan Indien occidental et austral, *Thesis,* Université Louis Pasteur, Strasbourg.

Goslin, J. & Patriat, P., 1984. Absolute and relative plate motions and hypotheses on the origin of five aseismic ridges in the Indian Ocean, *Tectonophysics,* **101,** 221–224.

Goslin, J., Recq, M. & Schlich, R., 1981. Structure profonde du plateau de Madagascar: relations avec le plateau de Crozet, *Tectonophysics,* **76,** 75–97.

Grégoire, M., Leyrit, H., Cottin, J.Y., Giret, A. & Mattielli, N., 1992. Les phases précoces et profondes du magmatisme des îles Kerguelen révélées par les enclaves basiques et ultrabasiques, *C. R. Acad. Sci. Paris,* **314,** 1203–1209.

Grégoire, M.H., Mattielli, N., Nicollet, C., Cottin, J.Y., Leyrit, H., Weis, D., Shimizu, N. & Giret, A., 1994. Oceanic mafic granulite xenoliths from the Kerguelen archipelago, *Nature,* **367,** 360–363.

Hales, A.L. & Nation, J.B., 1973. A seismic refraction study in the southern Indian Ocean, *Bull. seism. Soc. Am.*, **63,** 1951–1966.

Hess, H.H., 1955. Serpentines, orogeny and epeirogeny. *Geol. Soc. Am. Special Paper,* **65,** 391–408.

Hess, H.H., 1962. History of ocean basins, in *Petrological Studies,* Buddington volume, pp. 599–620, eds Engel, A.E.J. *et al.,* Geol. Soc. Am.

Houtz, R.E., Hayes, D.E. & Markl, R.G., 1977. Kerguelen Plateau bathymetry sediment distribution and crustal structure, *Mar. Geol.,* **25,** 95–130.

Hussong, D., Wipperman, L. & Kroenke, L.W., 1979. The crustal structure of the Ontong-Java and Manihiki plateaus, *J. geophys. Res.*, **84,** 6003–6010.

Kent, R., 1991. Lithospheric uplift in eastern Gondwana: evidence for a long-lived mantle plume system? *Geology,* **19,** 19–23.

Lameyre, J., Marot, A., Zimine, S., Cantagrel, J., Dosso, L., Giret, A. & Vidal, P., 1976. Chronological evolution of the Kerguelen islands syenite–granite ring complex. *Nature,* **263,** 306–307.

Lameyre, J., Marot, A., Zimine, S., Cantagrel, J., Dosso, L., Giret, A., Joron, J.L., Treuil, M. & Hottin, J., 1981. Etude géologique du complexe plutonique de la péninsule Rallier du Baty, îles Kerguelen. *Comb. natl. Fr. Res. Antarct.*, **49.**

Le Pichon, X. & Heirtzler, J., 1968. Magnetic anomalies in the Indian Ocean and sea-floor spreading, *J. geophys. Res.*, **73,** 2101–2117.

Le Roy, I., Recq, M., Goslin, J. & Charvis, P., 1993. Intraplate volcanism. The Mont Ross (Kerguelen Islands, southern Indian Ocean), EUG VII Strasbourg, *Terra abstracts,* **5,** 137.

Lewis, B.T.R., 1983. The process of formation of oceanic crust, *Science,* **220,** 151–157.

Lewis, B.T.R. & Snydsman, W.E., 1977. Evidence for a low velocity layer at the base of the oceanic crust, *Nature,* **266,** 340–344.

Li, Z.G., 1988. Structure, origine et évolution du plateau de Kerguelen, *Thesis,* Université Louis Pasteur, Strasbourg.

Ludwig, W.J., Nafe, J.E., Simpson, E.S.W. & Sacks, S., 1968. Seismic refraction measurements on the southeast continental margin, *J. geophys. Res.*, **73,** 3707–3719.

Marks, K.M. & Sandwell, D.T., 1991. Analysis of geoid height versus topography for oceanic plateaux and swells using nonbiased linear regression, *J. geophys. Res.*, **96,** 8045–8055.

Marot, A. & Zimine, S., 1981. Les complexes annulaires de syénites et granites alcalins dans la péninsule Rallier du Baty, îles Kerguelen (TAAF), *Com. natl. Fr. Res. Antarct.*, **49,** 15–114.

Matthews, D.H. & Davies, D., 1966. Geophysical studies of the Seychelles Bank, *Phil. Trans. Royal Soc. Lond.*, A, **259,** 227–239.

Mawson, D., 1934. The Kerguelen Archipelago, *The Geographical Journal,* London, **83**(1), 18–29.

McKenzie, D.P. & Bickle, M.J., 1988. The volume and composition of melt generated by extension of the lithosphere, *J. Petrology,* **29,** 625–679.

McKenzie, D.P. & Sclater, J.G., 1971. The evolution of the Indian Ocean since Late Cretaceous, *Geophys. J. R. astr. Soc.*, **25,** 457–528.

Montigny, R., Karpoff, A.M. & Hofmann, C., 1993. Résultats d'un dragage par 55°18′S–83°04′E dans le bassin de Labuan (campagne MD67, océan Indien méridional): implications géodynamiques, *Journées Spécialisées en géosciences marines, Soc. Géol. France,* 83.

Müller, R.D., Royer, J.Y. & Lawver, L.A., 1993. Revised plate motions relative to the hotspots from combined Atlantic and Indian Ocean hotspot track, *Geology,* **21,** 275–278.

Munschy, M. & Schlich, R., 1987. Structure and evolution of the Kerguelen–Heard Plateau (Indian Ocean) deduced from stratigraphic studies, *Mar. Geol.,* **76,** 131–152.

Munschy, M., Fritsch, B., Schlich, R., Fezga, F., Rotstein, Y. & Coffin, M., 1992. Structure and evolution of the Central Kerguelen Plateau deduced from seismic stratigraphic studies

and drilling at site 747, *Proc. Ocean Drilling Program, Sci. Res.*, **120,** 881–892.

Murray, J. & Renard, A.F., 1885. Reports of scientific results of the exploring voyage of HMS Challenger (1873–1876), in *Deep-Sea Deposits,* Longman, London.

Mutter, C. Z. & Mutter, J.C., 1993. Variations in thickness of layer 3 dominate oceanic crustal structure, *Earth planet. Sci. Lett.*, **117,** 295–317.

Nakamura, Y., Donoho, P.L., Roper, P.H. & McPherson, P., 1987. Large offset seismic surveying using ocean-bottom seismographs and air guns: instrumentation and field techniques, *Geophysics,* **52,** 1601–1611.

Nehlig, P. & Juteau, T., 1988. Deep crustal penetration and circulation at ocean ridges, evidences from the Oman ophiolite, *Mar. Geol.*, **84,** 209–228.

Nougier, J., 1970. Contribution à l'étude géologique et géomorphologique des îles Kerguelen (TAAF), *Com. Natl. Fr. Res. Antarct.*, **27.**

Operto, S., 1995. Structure et origine du Plateau de Kerguelen (Océan Indien austral): implications géodynamiques, *Thesis,* Université Pierre & Marie Curie, Paris.

Operto, S. & Charvis, P., 1995. Kerguelen Plateau; a volcanic passive fragment, *Geology,* **23,** 137–140.

Orcutt, J., Kennett, B., Dorman, L. & Prothero, W., 1975. A low velocity zone underlying a fast spreading ridge crest, *Nature,* **256,** 475–476.

Peirce, C. & Barton, P.J., 1991. Crustal structure of the Madeira-Tore Rise, eastern North Atlantic—results of a DOBS wide-angle and normal incidence seismic experiment in the Josephine Seamount region, *Geophys. J. Int.*, **106,** 357–378.

Ramsay, D.C., Colwell, J.B., Coffin, M.F., Davies, H.L., Hill, P.J., Pigram, C.J. & Stagg, H.M.J., 1986. New findings from the Kerguelen Plateau, *Geology,* **14,** 589–593.

Recq, M., 1983. Anomalies isostatiques sous le bassin de Crozet et la dorsale est-indienne. *Bull. Soc. géol. Fr.,* **XXV**(6), 963–972.

Recq, M., 1991. Underplating below and adjacent to the Kerguelen archipelago. EUG VI, Strasbourg, *Terra abstracts,* **3**(1), 272.

Recq, M. & Charvis, P., 1987. La ride asismique de Kerguelen–Heard: anomalie du géoïde et compensation isostatique, *Mar. Geol.*, **76,** 301–311.

Recq, M. & Charvis, P., 1987. La ride asismique de Kerguelen–Heard: anomalie due géoïde et compensation isostatique, *Mar. Geol.*, **76,** 301–311.

Recq, M. & Goslin, J., 1981. Etude de l'équilibre isostatique dans le Sud-Ouest de l'océan Indien à l'aide des résultats de réfraction sismique, *Mar. Geol.*, **41,** M1–M10.

Recq, M., Charvis, P. & Hirn, A., 1983. Premières données sur la structure profonde de la ride de Kerguelen, d'après la réfraction sismique, *C.R. Acad. Sci., Paris,* **297,** 903–908.

Recq, M., Brefort, D., Malod, J. & Veinante, J.L., 1990. The Kerguelen Isles (southern Indian Ocean). New results on deep structure from refraction profiles, *Tectonophysics,* **182,** 227–248.

Recq, M., Whitmarsh, R.B. & Sibuet, J.C., 1991. Anatomy of a lherzolite ridge, Galicia margin. EUG VI, Strasbourg, *Terra abstracts,* **3**(1), 273.

Recq, M., Le Roy, I., Goslin, J., Charvis, P. & Brefort, D., 1994. Structure profonde du Mont Ross d'après la réfraction sismique (îles Kerguelen, océan Indien austral), *Can. J. Earth Sci.*, **31,** 1806–1821.

Rotstein, Y., Schaming, M., Schlich, R. & Colwell, J.B., 1990. Basin evolution in oceanic volcanic plateaux: seismic reflection evidence from the Kerguelen Plateau, South Indian Ocean, *Mar. Petrol. Geol.*, **7,** 2–12.

Rouillon, G., 1963. *Cartes des Anomalies gravimétriques des îles Kerguelen et Crozet,* Terres Australes et Antarctiques Françaises.

Royer, J.Y. & Coffin, M., 1992. Jurassic to Eocene plate tectonic reconstruction of the Kerguelen Plateau region, in *Proc. ODP, Sci. Results, 120,* pp. 917–928, eds Wise, S.W. Jr. *et al.*, College Station, TX (Ocean Drilling Program).

Ryall, A. & Bennett, D.L., 1968. Crustal structure of southern Hawaii related to volcanic processes in the upper mantle, *J. geophys. Res.*, **73,** 4561–4582.

Salisbury, M.H. & Christensen, N.I., 1978. The seismic velocity structure of a traverse through the Bay of Islands ophiolite complex, Newfoundland, an exposure of oceanic crust and upper mantle, *J. geophys. Res.*, **83,** 805–817.

Saunders, A.D., Storey, M., Kent, R. & Gibson, I.L., 1990. The Kerguelen hotspot: the history of a long-lived mantle plume system, *Soc. géol. de France, A Tribute to Professeur Jean Lameyre.* Paris, 26–27 Novembre 1990.

Schaming, M. & Rotstein, Y., 1990. Basement reflectors in the Kerguelen Plateau, south Indian Ocean: Indications for the structure and early history of the plateau, *Geol. Soc. Am. Bull.*, **102,** 580–592.

Schlich, R., 1975. Structure et âge de l'océan Indien occidental, *Com. natl. Fr. Rech. Antarct.*, **38.**

Schlich, R., 1982. The Indian Ocean: aseismic ridges, spreading centres, and ocean basins, in *The Ocean Basins and Margins,* vol. 6: *The Indian Ocean,* pp. 51–147, eds Nairn, A.E.G. & Stehli, F.G., Plenum, New York.

Schlich, R. *et al.,* 1974. Site 246 and 247, in *Initial Reports of the Deep Sea Drilling Project,* US Government Printing Office, Washington, DC, **25,** 237–257.

Schlich, R., Coffin, M.F., Munschy, M., Stagg, H.M.J., Li, Z.G. & Revill, K., 1987. Bathymetric chart of the Kerguelen Plateau, jointly edited by Bureau of Mineral Resources, Geology and Geophysics, Canberra, Australia, Institut de Physique du Globe, Strasbourg, and Terres Australes et Antarctiques Françaises, Paris, France.

Sinha, M.C., Louden, K.E. & Parsons, B., 1981. The crustal structure of the Madagascar Ridge, *Geophys. J. R. astr. Soc.*, **66,** 351–377.

Souriau, A., 1981. The upper mantle beneath Ninetyeast Ridge and Broken Ridge, Indian Ocean, from surface waves, *Geophys. J. R. astr. Soc.*, **67,** 359–374.

Spence, G.D., Whittall, K.P. & Clowes, R.M., 1984. Practical synthetic seismograms for laterally varying media calculated by asymptotic ray theory, *Bull. seism. Soc. Am.*, **74,** 1209–1223.

Stephenson, P.J., 1964. Some geological observations on Heard Island, in *Antarctic Geology,* pp. 14–23, ed. Adie, R.J., North Holland, Amsterdam.

Storey, M., Saunders, A.D., Tarney, J., Leaf, P., Thirlwall, M.F., Thompson, R.N., Menzies, M.A. & Marriner, G.F., 1988. Geochemical evidence for plume–mantle interactions beneath Kerguelen and Heard Islands, Indian Ocean, *Nature,* **336,** 371–374.

Storey, M., Saunders, A.D., Tarney, J., Gibson, I.L., Norry, M.J., Thirlwall, M.F., Leaf, P., Thompson, R.N. & Menzies, M.A., 1989. Contamination of Indian Ocean asthenosphere by the Kerguelen–Heard mantle plume, *Nature,* **338,** 574–576.

Storey, M., Kent, R.W., Saunders, A.D., Salters, V.J.M., Hergt, H., Whitechurch, H., Sevigny, J.H., Thirlwall, M.F., Leat, P., Ghose, N.C. & Gifford, M., 1992. Lower Cretaceous volcanic rocks on continental margins and their relationship to the Kerguelen Plateau, *Proc. Ocean Drilling Program, Sci. Res.*, **120,** 33–47.

Ten Brink, U.S. & Brocher, T.M., 1987. Multichannel seismic evidence for a subcrustal intrusive complex under Ohau and a model for Hawaiian volcanism, *J. geophys. Res.*, **92,** 13 687–13 707.

Watkins, N.D., Gunn, B.M., Nougier, J. & Baski, A.K., 1974. Kerguelen: continental fragment or oceanic island? *Geol. Soc. Am. Bull.*, **85,** 201–212.

Watts, A.B. & ten Brink, U.S., 1989. Crustal structure, flexure, and

subsidence history of the Hawaiian Islands, *J. geophys. Res.*, **94,** 10 473–10 500.

Watts, A.B., ten Brink, U.S., Buhl, P. & Brocher, T.M., 1985. A multichannel seismic study of lithospheric flexure across the Hawaiian–Emperor seamount chain, *Nature,* **315,** 105–111.

White, R.S., 1992. Crustal structure of North Atlantic continental margins, *J. geol. Soc., Lond.,* **149,** 841–854.

White, R.S. & McKenzie, D.P., 1989. Magmatism at rift zones: the generation of volcanic continental margins and flood basalts, *J. geophys. Res.,* **94,** 7685–7729.

White, R.S., Spence, G.D., Fowler, S.R., McKenzie, D.P., Westbrook, G.K. & Bowen, A.N., 1987. Magmatism at rifted continental margins, *Nature,* **330,** 439–444.

White, R.S. & McKenzie, D.P. & O'Nions, R.K., 1992. Oceanic crustal thickness from seismic measurements and rare earth element inversions, *J. geophys. Res.,* **97,** 19 683–19 715.

Whitechurch, H., Montigny, R., Sevigny, J.H., Storey, M. & Salters, V.J.M., 1992. K–Ar and $^{40}Ar/^{39}Ar$ ages of central Kerguelen Plateau basalts, *Proc. Ocean Drilling Program, Sci. Res.,* **120,** 71–77.

Whitmarsh, R.B., Avedik, F. & Saunders, M.R., 1986. The seismic structure of thinned continental crust in the northern Bay of Biscay, *Geophys. J. R. astr. Soc.,* **86,** 589–602.

Whitmarsh, R.B., Pinheiro, L.M., Miles, P.R., Recq, M. & Sibuet, J.C., 1993. Thin crust at the western Iberia ocean–continent transition and ophiolites, *Tectonics,* **12,** 1230–1239.

Wicquart, E. & Fröhlich, F., 1986. La sédimentation du plateau de Keguelen–Heard. Relations avec l'évolution de l'océan Indien au Cénozoïque, *Bull. Soc. géol. France,* **4,** 569–574.

Zelt, C.A. & Smith, R.B., 1992. Seismic traveltime inversion for 2-D crustal velocity structure, *Geophys. J. Int.,* **108,** 16–34.

Zucca, B.J., Hill, D.P. & Kovach, R.L., 1982. Crustal structure of Mauna Loa volcano, Hawaii, from seismic refraction and gravity data, *Bull. seism. Soc. Am.,* **72,** 1535–1550.